where f and i represent the frequency (Hz) and imaginary units, respectively; K_N is the neural arc gain; f_C is the frequency (Hz) for a derivative characteristic; L_N is lag time (s).

The peripheral arc transfer function $[G_P(f)]$ using a second-order low-pass filter can be expressed as

$$G_P(f) = \frac{K_P}{1 + 2\zeta \frac{f}{f_N} i + \left(\frac{f}{f_N} i\right)^2} \exp(-2\pi f i L_P)$$

where K_P, f_N, ζ, and L_P represent the peripheral arc gain, natural frequency (Hz), damping ratio, and lag time (s), respectively.

The transfer function of the total baroreflex loop is expressed as the product of the neural and peripheral arc transfer functions.

$$G_{AP}(f) = G_N(f) \cdot G_P(f)$$

The gain and lag time of the total baroreflex loop is expressed as $K = K_N \cdot K_P$ and $L = L_N + L_P$. The parameters of the model response were set at $K = 1.0$, $f_C = 0.12$, $L_N = 0.55$, $f_N = 0.071$, $\zeta = 1.37$, and $L_P = 1.0$ according to previous data.[15]

Model of Baroreflex Under Closed-Loop AP Response

The baroreflex system under the closed-loop AP input to HR response was modeled (Fig. 8a).

$$HR_{change}(f) = G_{HR}(f) \cdot AP_{change}(f)$$

The pressure change $[AP_{change}(f)]$ to the exogenous perturbation $[AP_{noise}(f)]$ is the sum of the feedback signal and perturbation under closed-loop condition.[15] G_{HR} is the transfer function under the carotid sinus open loop in the cardiac baroreflex (CSP input and HR output).

$$AP_{change}(f) = G_{AP}(f) \cdot AP_{change}(f) + AP_{noise}(f)$$

Rearranging above equation with respect to $AP_{change}(f)$ yields

$$AP_{change}(f) = \frac{AP_{noise}(f)}{1 - G_{AP}(f)}$$

The time integral of the inverse Fourier transform of $AP_{change}(f)$ is the AP change to an exogenous step perturbation. G_{AP} is the transfer function under the carotid sinus open loop for the total baroreflex. The AP_{change} and HR_{change} can be simply observed by the monitoring system. The transfer function between the HR and AP responses was excluded because of the insignificant relationship as previously indicated.[22]

The transfer functions, G_{AP} and G_{HR}, were approximated using a first-order low-pass filter.

$$G(f) = \frac{-K}{\left(1 + \frac{f}{f_C} i\right)} \cdot \exp(-2\pi f i L)$$

The parameters of the transfer functions were set at $K = 1.03$, $f_C = 0.018$, and $L = 1.34$ for the total loop (Fig. 8a, G_{AP}); $K = 0.51$, $f_C = 0.049$, and $L = 1.14$ for the cardiac baroreflex (G_{HR}), according to previous data.[20]

ACKNOWLEDGMENTS

REFERENCES

[1]Ando, S., H. R. Dajani, B. L. Senn, G. E. Newton, and J. S. Floras. Sympathetic alternans. Evidence for arterial baroreflex control of muscle sympathetic nerve activity in congestive heart failure. *Circulation* 95:316–319, 1997.
[2]Burgess, D. E., D. C. Randall, R. O. Speakman, and D. R. Brown. Coupling of sympathetic nerve traffic and BP at very low frequencies is mediated by large-amplitude events. *Am. J. Physiol. Regul. Integr. Comp. Physiol.* 284:R802–R810, 2003.
[3]Dampney, R. A. Functional organization of central pathways regulating the cardiovascular system. *Physiol. Rev.* 74:323–364, 1994.
[4]Davrath, L. R., Y. Goren, I. Pinhas, E. Toledo, and S. Akselrod. Early autonomic malfunction in normotensive individuals with a genetic predisposition to essential hypertension. *Am. J. Physiol. Heart Circ. Physiol.* 285:H1697–H1704, 2003.
[5]Eckberg, D. L., and T. A. Kuusela. Human vagal baroreflex sensitivity fluctuates widely and rhythmically at very low frequencies. *J. Physiol.* 567:1011–1019, 2005. doi:10.1113/jphysiol.2005.091090.
[6]Ellenbogen, K. A., P. K. Mohanty, S. Szentpetery, and M. D. Thames. Arterial baroreflex abnormalities in heart failure: reversal after orthotopic cardiac transplantation. *Circulation* 79:51–58, 1989.
[7]Fadel, P. J., S. Ogoh, D. M. Keller, and P. B. Raven. Recent insights into carotid baroreflex function in humans

using the variable pressure neck chamber. *Exp. Physiol.* 88:671–680, 2003. doi:10.1113/eph8802650.

[8]Fadel, P. J., M. Stromstad, D. W. Wray, S. A. Smith, P. B. Raven, and N. H. Secher. New insights into differential baroreflex control of heart rate in humans. *Am. J. Physiol. Heart Circ. Physiol.* 284:H735–H743, 2003.

[9]Glantz, S. A. Primer of Biostatistics. 4th ed. New York: McGraw Hill, 1997.

[10]Grassi, G., C. Turri, G. Seravalle, G. Bertinieri, A. Pierini, and G. Mancia. Effects of chronic clonidine administration on sympathetic nerve traffic and baroreflex function in heart failure. *Hypertension* 38:286–291, 2001. doi:10.1161/hy1201.096117.

[11]Grossmann, A., R. Kronland-Martinet, and J. Morlet. Reading and understanding continuous wavelets transforms. In: Wavelets, Time-Frequency Methods and Phase Space, edited by J. M. Combes, A. Grossmann, and P. Tchamitchian. Berlin: Springer, 1989, pp. 2–20.

[12]Guyton, A. C., T. G. Coleman, and H. J. Granger. Circulation: overall regulation. *Annu. Rev. Physiol.* 34:13–46, 1972. doi:10.1146/annurev.ph.34.030172.000305.

[13]Hayano, J., J. A. Taylor, S. Mukai, A. Okada, Y. Watanabe, K. Takata, and T. Fujinami. Assessment of frequency shifts in R-R interval variability and respiration with complex demodulation. *J. Appl. Physiol.* 77:2879–2888, 1994.

[14]Ichinose, M., M. Saito, N. Kondo, and T. Nishiyasu. Time-dependent modulation of arterial baroreflex control of muscle sympathetic nerve activity during isometric exercise in humans. *Am. J. Physiol. Heart Circ. Physiol.* 290:H1419–H1426, 2006. doi:10.1152/ajpheart.00847.2005.

[15]Ikeda, Y., T. Kawada, M. Sugimachi, O. Kawaguchi, T. Shishido, T. Sato, H. Miyano, W. Matsuura, J. Alexander, Jr., and K. Sunagawa. Neural arc of baroreflex optimizes dynamic pressure regulation in achieving both stability and quickness. *Am. J. Physiol. Heart Circ. Physiol.* 271:H882–H890, 1996.

[16]Jordan, J., H. R. Toka, K. Heusser, O. Toka, J. R. Shannon, J. Tank, A. Diedrich, C. Stabroth, M. Stoffels, R. Naraghi, W. Oelkers, H. Schuster, H. P. Schobel, H. Haller, and F. C. Luft. Severely impaired baroreflex-buffering in patients with monogenic hypertension and neurovascular contact. *Circulation* 102:2611–2618, 2000.

[17]Kashihara, K. Automatic regulation of hemodynamic variables in acute heart failure by a multiple adaptive predictive controller based on neural networks. *Ann. Biomed. Eng.* 34:1846–1869, 2006. doi:10.1007/s10439-006-9190-9.

[18]Kashihara, K., T. Kawada, M. Li, M. Sugimachi, and K. Sunagawa. Bezold-Jarisch reflex induced by phenylbiguanide lowers arterial pressure mainly via the downward shift of the baroreflex neural arc. *Jpn. J. Physiol.* 54:395–404, 2004. doi:10.2170/jjphysiol.54.395.

[19]Kashihara, K., T. Kawada, K. Uemura, M. Sugimachi, and K. Sunagawa. Adaptive predictive control of arterial blood pressure based on a neural network during acute hypotension. *Ann. Biomed. Eng.* 32:1365–1383, 2004. doi:10.1114/B:ABME.0000042225.19806.34.

[20]Kashihara, K., T. Kawada, Y. Yanagiya, K. Uemura, M. Inagaki, H. Takaki, M. Sugimachi, and K. Sunagawa. Bezold-Jarisch reflex attenuates dynamic gain of baroreflex neural arc. *Am. J. Physiol. Heart Circ. Physiol.* 285:H833–H840, 2003.

[21]Kashihara, K., Y. Takahashi, K. Chatani, T. Kawada, C. Zheng, M. Li, M. Sugimachi, and K. Sunagawa. Intravenous angiotensin II does not affect dynamic baroreflex characteristics of the neural or peripheral arc. *Jpn. J. Physiol.* 53:135–143, 2003. doi:10.2170/jjphysiol.53.135.

[22]Kawada, T., T. Miyamoto, K. Uemura, K. Kashihara, A. Kamiya, M. Sugimachi, and K. Sunagawa. Effects of neuronal norepinephrine uptake blockade on baroreflex neural and peripheral arc transfer characteristics. *Am. J. Physiol. Regul. Integr. Comp. Physiol.* 286:R1110–1120, 2004. doi:10.1152/ajpregu.00527.2003.

[23]Kawada, T., Y. Yanagiya, K. Uemura, T. Miyamoto, C. Zheng, M. Li, M. Sugimachi, and K. Sunagawa. Input-size dependence of the baroreflex neural arc transfer characteristics. *Am. J. Physiol. Heart Circ. Physiol.* 284:H404–H415, 2003.

[24]Kent, B. B., J. W. Drane, B. Blumenstein, and J. W. Manning. A mathematical model to assess changes in the baroreceptor reflex. *Cardiology* 57:295–310, 1972.

[25]Landesberg, G., D. Adam, Y. Berlatzky, and S. Akselrod. Step baroreflex response in awake patients undergoing carotid surgery: time- and frequency-domain analysis. *Am. J. Physiol.* 274:H1590–H1597, 1998.

[26]Lee, D. Coherent oscillations in neuronal activity of the supplementary motor area during a visuomotor task. *J. Neurosci.* 23:6798–6809, 2003.

[27]Lipman, R. D., J. K. Salisbury, and J. A. Taylor. Spontaneous indices are inconsistent with arterial baroreflex gain. *Hypertension* 42:481–487, 2003. doi:10.1161/01.HYP.0000091370.83602.E6.

[28]Liu, H. K., S. J. Guild, J. V. Ringwood, C. J. Barrett, B. L. Leonard, S. K. Nguang, M. A. Navakatikyan, and S. C. Malpas. Dynamic baroreflex control of blood pressure: influence of the heart vs. peripheral resistance. *Am. J. Physiol. Regul. Integr. Comp. Physiol.* 283:R533–R542, 2002.

[29]Lucini, D., M. Pagani, G. S. Mela, and A. Malliani. Sympathetic restraint of baroreflex control of heart period in normotensive and hypertensive subjects. *Clin. Sci. (Lond.)* 86:547–556, 1994.

[30]Malliani, A., M. Pagani, F. Lombardi, and S. Cerutti. Cardiovascular neural regulation explored in the frequency domain. *Circulation* 84:482–492, 1991.

[31]Marmarelis, P. Z., and V. Z. Marmarelis. The white noise method in system identification. In: Analysis of Physiological Systems. New York: Plenum, 1978, pp. 131–221.

[32]Masaki, H., T. Imaizumi, Y. Harasawa, and A. Takeshita. Dynamic arterial baroreflex in rabbits with heart failure induced by rapid pacing. *Am. J. Physiol.* 267:H92–H99, 1994.

[33]Mohrman, D. E., and L. J. Heller. Cardiovascular Physiology. 4th ed. New York: McGraw-Hill, 1997.

[34]Motard, R. L., and B. Joseph. Wavelet Applications in Chemical Engineering. Boston: Kluwer Academic Publishers, 1994.

[35]Munakata, M., Y. Imai, H. Takagi, M. Nakao, M. Yamamoto, and K. Abe. Altered frequency-dependent characteristics of the cardiac baroreflex in essential hypertension. *J. Auton. Nerv. Syst.* 49:33–45, 1994. doi:10.1016/0165-1838(94)90018-3.

[36]Osculati, G., G. Grassi, C. Giannattasio, G. Seravalle, F. Valagussa, A. Zanchetti, and G. Mancia. Early alterations of the baroreceptor control of heart rate in patients with acute myocardial infarction. *Circulation* 81:939–948, 1990.

[37]Parati, G., M. DiRienzo, and G. Mancia. Dynamic modulation of baroreflex sensitivity in health and disease. *Ann. NY Acad. Sci.* 940:469–487, 2001.

[38]Parati, G., J. P. Saul, and P. Castiglioni. Assessing arterial baroreflex control of heart rate: new perspectives. *J. Hypertens.* 22:1259–1263, 2004. doi:10.1097/01.hjh.0000125469.35523.32.

[39]Parmer, R. J., J. H. Cervenka, and R. A. Stone. Baroreflex sensitivity and heredity in essential hypertension. *Circulation* 85:497–503, 1992.

[40]Persson, P. B., M. DiRienzo, P. Castiglioni, C. Cerutti, M. Pagani, N. Honzikova, S. Akselrod, and G. Parati. Time versus frequency domain techniques for assessing baroreflex sensitivity. *J. Hypertens.* 19:1699–1705, 2001. doi:10.1097/00004872-200110000-00001.

[41]Pinna, G. D., R. Maestri, G. Raczak, and M. T. La Rovere. Measuring baroreflex sensitivity from the gain function between arterial pressure and heart period. *Clin. Sci. (Lond.)* 103:81–88, 2002.

[42]Pitzalis, M. V., F. Mastropasqua, A. Passantino, F. Massari, L. Ligurgo, C. Forleo, C. Balducci, F. Lombardi, and P. Rizzon. Comparison between noninvasive indices of baroreceptor sensitivity and the phenylephrine method in post-myocardial infarction patients. *Circulation* 97:1362–1367, 1998.

[43]Porta, A., G. Baselli, O. Rimoldi, A. Malliani, and M. Pagani. Assessing baroreflex gain from spontaneous variability in conscious dogs: role of causality and respiration. *Am. J. Physiol. Heart Circ. Physiol.* 279:H2558–H2567, 2000.

[44]Radaelli, A., L. Bernardi, F. Valle, S. Leuzzi, F. Salvucci, L. Pedrotti, E. Marchesi, G. Finardi, and P. Sleight. Cardiovascular autonomic modulation in essential hypertension. Effect of tilting. *Hypertension* 24:556–563, 1994.

[45]Rudas, L., A. A. Crossman, C. A. Morillo, J. R. Halliwill, K. U. Tahvanainen, T. A. Kuusela, and D. L. Eckberg. Human sympathetic and vagal baroreflex responses to sequential nitroprusside and phenylephrine. *Am. J. Physiol.* 276:H1691–H1698, 1999.

[46]Sagawa, K. Baroreflex control of systemic arterial pressure and vascular bed. In: Handbook of Physiology. The Cardiovascular System. Peripheral Circulation and Organ Blood Flow, sect. 2, vol. III, pt. 2, chap. 14. Bethesda, MD: Am. Physiol. Soc., 1983, pp. 453–496.

[47]Sato, T., T. Kawada, M. Inagaki, T. Shishido, H. Takaki, M. Sugimachi, and K. Sunagawa. New analytic framework for understanding sympathetic baroreflex control of arterial pressure. *Am. J. Physiol.* 276:H2251–H2261, 1999.

[48]Sinkkonen, J., H. Tiitinen, and R. Naatanen. Gabor filters: an informative way for analysing event-related brain activity. *J. Neurosci. Methods* 56:99–104, 1995. doi:10.1016/0165-0270(94)00111-S.

[49]Tallon-Baudry, C., O. Bertrand, C. Delpuech, and J. Pernier. Stimulus specificity of phase-locked and non-phase-locked 40 Hz visual responses in human. *J. Neurosci.* 16:4240–4249, 1996.

[50]Toledo, E., O. Gurevitz, H. Hod, M. Eldar, and S. Akselrod. Wavelet analysis of instantaneous heart rate: a study of autonomic control during thrombolysis. *Am. J. Physiol. Regul. Integr. Comp. Physiol.* 284:R1079–R1091, 2003.

[51]Westerhof, B. E., J. Gisolf, J. M. Karemaker, K. H. Wesseling, N. H. Secher, and J. J. van Lieshout. Time course analysis of baroreflex sensitivity during postural stress. *Am. J. Physiol. Heart Circ. Physiol.* 291:H2864–H2874, 2006. doi:10.1152/ajpheart.01024.2005.

[52]Zhang, R., K. Behbehani, C. G. Crandall, J. H. Zuckerman, and B. D. Levine. Dynamic regulation of heart rate during acute hypotension: new insight into baroreflex function. *Am. J. Physiol. Heart Circ. Physiol.* 280:H407–H419, 2001.

Electroacupuncture changes the relationship between cardiac and renal sympathetic nerve activities in anesthetized cats

Hiromi Yamamoto [a,*], Toru Kawada [b], Atsunori Kamiya [b], Toru Kita [a], Masaru Sugimachi [b]

[a] Department of Cardiovascular Medicine, Graduate School of Medicine, Kyoto University, Kyoto 606-8501, Japan
[b] Department of Cardiovascular Dynamics, Advanced Medical Engineering Center, National Cardiovascular Center Research Institute, Osaka 565-8565, Japan

Electroacupuncture changes the relationship between cardiac and renal sympathetic nerve activities in anesthetized cats

Hiromi Yamamoto [a,*], Toru Kawada [b], Atsunori Kamiya [b], Toru Kita [a], Masaru Sugimachi [b]

[a] Department of Cardiovascular Medicine, Graduate School of Medicine, Kyoto University, Kyoto 606-8501, Japan
[b] Department of Cardiovascular Dynamics, Advanced Medical Engineering Center, National Cardiovascular Center Research Institute, Osaka 565-8565, Japan

ARTICLE INFO

ABSTRACT

Electroacupuncture (EA) is known to affect hemodynamics through modulation of efferent sympathetic nerve activity (SNA), however, possible regional differences in the SNA response to EA remains to be examined. Based on the discordance between arterial blood pressure and heart rate changes during EA, we hypothesized that regional differences would occur among SNAs during EA. To test this hypothesis, we compared changes in cardiac and renal SNAs in response to 1-min EA (10 Hz or 2 Hz) of a hind limb in adult cats anesthetized with pentobarbital sodium. Renal SNA remained decreased for 1 min during EA ($P<0.01$ for both 10 Hz and 2 Hz). In contrast, cardiac SNA tented to decrease only in the beginning of EA. It increased during the end of EA ($P<0.05$ for 2 Hz) and further increased after the end of EA ($P<0.01$ both for 10 Hz and 2 Hz). There was a quasi-linear relationship between renal and cardiac SNAs with a slope of 0.69 (i.e., renal SNA was more suppressed than cardiac SNA) during the last 10 s of EA. The discrepancy between the renal and cardiac SNAs persisted after sinoaortic denervation and vagotomy. In conclusion, EA evokes differential patterns of SNA responses and changes the relationship between cardiac and renal SNAs.

© 2008 Elsevier B.V. All rights reserved.

1. Introduction

Electroacupuncture stimulation has been used to modulate autonomic nervous activity and cardiovascular function (Kimura and Sato, 1997; Lin et al., 2001). Several studies have demonstrated that arterial blood pressure (AP) is decreased by acupuncture-like stimulation in anesthetized animals (Kline et al., 1978; Ku and Zou, 1993; Lee and Kim, 1994; Zhou et al., 2005). The cardiovascular responses induced by acupuncture-like stimulation are reflexes mediated via somatic afferent nerves and autonomic efferent nerves (Sato et al., 1994, 2002). Although slow-onset, long-lasting effects may be characteristics of acupuncture, rapid-onset, short-lasting effects are also reported in some experimental conditions. In anesthetized rats, Ohsawa et al. (1995) reported that acupuncture-like stimulation of a hind limb decreased AP in association with a decrease in renal sympathetic nerve activity (RSNA). Uchida et al. (2007) reported that acupuncture-like stimulation of a hind limb induced decreases in cardiac sympathetic nerve activity (CSNA) and heart rate (HR). On the other hand, Kobayashi et al. (1998) reported that acupuncture stimulation produced variable responses including tachycardia, bradycardia, or no responses. We hypothesized that regional differences in sympathetic nerve activities would account for the diverse HR response and more consistent hypotensive response reported during EA. Although Sato et al. (1981) reported that stimulation of group III muscle afferent fibers of a hind limb induces either bradycardic or tachycardic response in anesthetized cats, they did

not measure efferent sympathetic nerve activities. To test the hypothesis that EA would evoke regional differences among sympathetic efferent nerve activities, we simultaneously recorded and directly compared CSNA and RSNA during EA in anesthetized cats. The kidneys are important for a long-term AP control via the maintenance of sodium and water balance (DiBona, 2005). At the same time, because the kidneys receive approximately 20% of the cardiac output in resting humans (Rowell, 1974), we thought changes in RSNA could contribute to the acute AP control. We first examined changes in AP, HR, CSNA, and RSNA in response to 10-Hz or 2-Hz EA of a hind limb. We then investigated possible roles of arterial baroreflex and vagal nerve activities in the effects of EA using sinoaortic denervation and vagotomy.

2. Methods

2.1. Surgical preparation

Animal care was provided in strict accordance with the Guiding Principles for the Care and Use of Animals in the Field of Physiological Sciences approved by the Physiological Society of Japan. All protocols were approved by the Animal Subject Committee of National Cardiovascular Center. Adult cats weighing 3.0 to 5.2 kg were anesthetized by an intraperitoneal injection of pentobarbital sodium (30–35 mg/kg) and ventilated mechanically via a tracheal tube with oxygen-supplied room air. The depth of anesthesia was maintained with a continuous intravenous infusion of pentobarbital sodium ($1-2$ mg·kg^{-1}·h^{-1}) through a catheter inserted into the right femoral vein. Vecuronium bromide (0.5–

---

* Corresponding author. Tel.: +81 75 751 3195; fax: +81 75 751 3203.
E-mail address: hiromi@kuhp.kyoto-u.ac.jp (H. Yamamoto).

1.0 mg·kg^{-1}·h^{-1}, i.v.) was given continuously to suppress muscular activity. AP was measured using a catheter-tip manometer inserted from the right femoral artery and advanced into the thoracic aorta. A pair of bipolar stainless steel wire electrodes (AS633, Cooner Wire, Chatsworth, CA) was attached to a branch of the left renal nerve through a flank incision. The nerve fibers peripheral to the electrodes were tightly ligated and crushed to remove afferent signals from the kidney. The nerve fibers and the electrodes were secured with silicone glue (Kwik-Sil, World Precision Instruments, Sarasota, FL). Another pair of bipolar stainless steel wire electrodes was attached to a branch of the left cardiac sympathetic nerve arising from the left stellate ganglion through a resection of the left second rib. The nerve fibers distal to the electrodes were sectioned to eliminate afferent signals from the heart. The nerve fibers and the electrodes were secured with silicone glue. Because the influence of the right cardiac sympathetic nerve on sinus rhythm is greater than that of he left cardiac sympathetic nerve (Yasunaga and Nosaka, 1979), we kept the right cardiac sympathetic nerve intact to preserve the HR response to EA. One rationale for recording left CSNA was that there was no significant laterality in left and right CSNAs during sympathetic perturbation via the arterial baroreflex (Kawada et al., 2003). The preamplified nerve activity signals were band-pass-filtered between 150 and 1000 Hz and then rectified and low-pass-filtered with a cut-off frequency of 30 Hz to quantify CSNA and RSNA. For sinoaortic denervation and vagotomy, we sectioned all nerves surrounding the common carotid arteries at the neck. The carotid sinus nerves were crushed by tight ligatures of 3-0 silk suture around tissues between the internal and external carotid arteries.

2.2. Electroacupuncture

In the supine position, both hind limbs were lifted to obtain a better view of the lateral sides of the lower legs. An EA needle with a diameter of 0.2 mm (CE0123, Seirin-Kasei, Japan) was inserted into a point below the knee joint just lateral to the tibia to the depth of approximately 10 mm. Another EA needle was inserted into the skin behind the ankle as the ground. EA was applied to either the left or right leg using an isolator connected to an electrical stimulator (SEN 7203, Nihon Kohden, Japan). The pulse width was set at 500 μs and the stimulus frequency was set at either 10 or 2 Hz. The stimulus current was set in the range from 2 to 5 mA (2.9±1.1 mA, mean±SD) to produce an AP decrease of more than 5 mmHg at 10-Hz stimulation.

2.3. Protocols

Protocol 1. To examine regional differences in sympathetic nerve activities, we applied 10-Hz or 2-Hz EA for 1 min while measuring AP, HR, CSNA, and RSNA. EA was applied to either the left or right hind limb in random order. An interval of at least 5 min was allowed between the EA trials.

Protocol 2. We applied 10-Hz electrical stimulation to a nonspecific control point in the front of the right thigh to examine whether changes in AP, HR, CSNA, and RSNA observed in Protocol 1 were caused by nonspecific responses to the electrical stimulation.

Protocol 3. To examine possible roles of arterial baroreflex and vagal nerve activities in the effects of EA, we performed sinoaortic denervation and vagotomy. Approximately 20 min after the sinoaortic denervation and vagotomy, changes in AP, HR, CSNA, and RSNA in response to 10-Hz EA were examined.

Protocol 4. To confirm baroreflex-induced changes in sympathetic nerve activity, changes in CSNA and RSNA in response to an intravenous phenylephrine injection (5 μg/kg) were examined before performing sinoaortic denervation and vagotomy. CSNA and
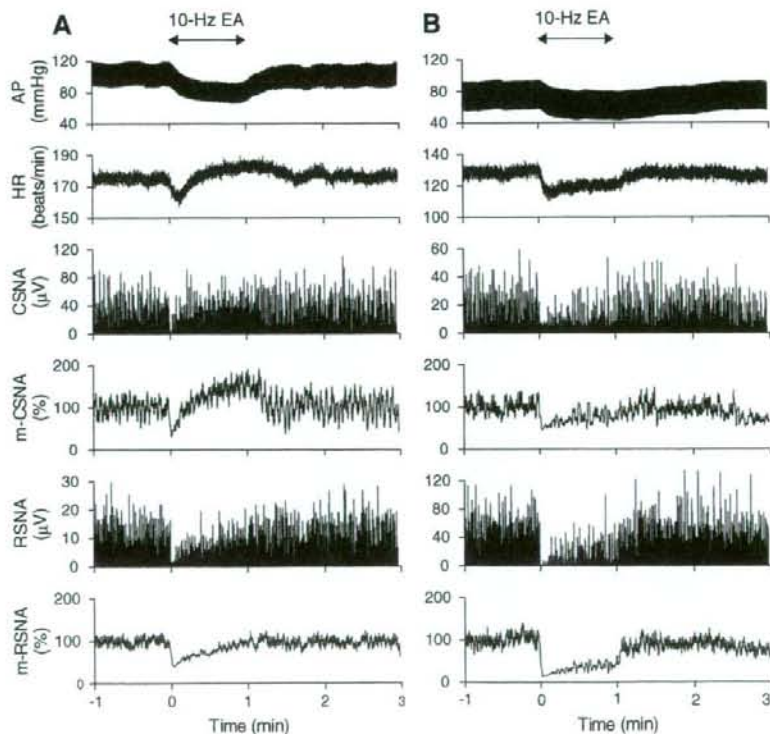
Fig. 1. Time series of arterial pressure (AP), heart rate (HR), cardiac sympathetic nerve activity (CSNA), 2-s moving averaged CSNA (m-CSNA), renal sympathetic nerve activity (RSNA), and 2-s moving averaged RSNA (m-RSNA) during 10-Hz electroacupuncture (EA) obtained from two different animals (see main text for details).
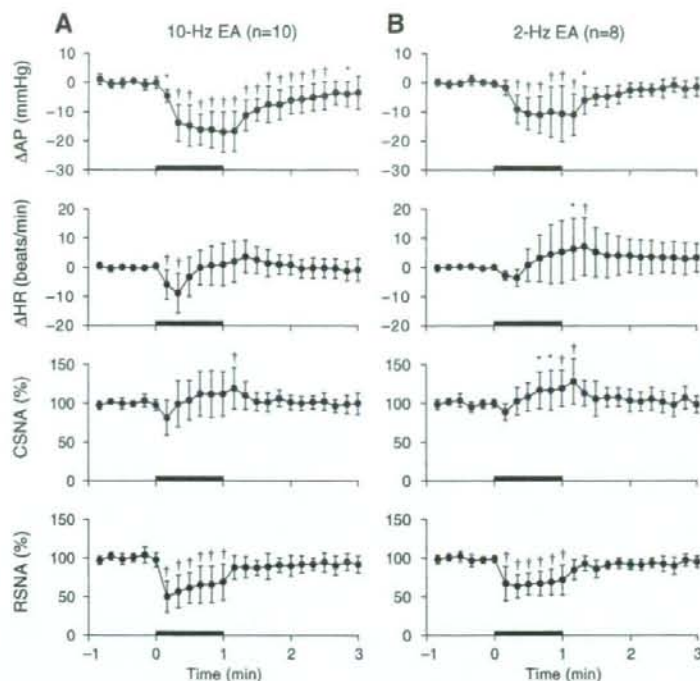
Fig. 2. Changes in arterial pressure (ΔAP), changes in heart rate (ΔHR), percent values of cardiac sympathetic nerve activity (CSNA), and percent values of renal sympathetic nerve activity (RSNA) during 10-Hz electroacupuncture (EA) (A) and 2-Hz EA (B) averaged for all trials. Values are the mean ±SD. *P<0.05 and †P<0.01 from the first data point during the pre-EA baseline period.

RSNA were expected to be decreased by phenylephrine-induced hypertension.

2.4. Data analysis

Data were digitized by a 16-bit analog-to-digital converter (Contec, Japan) and stored at 200 Hz in a dedicated laboratory computer system. Because the absolute voltage of nerve activity varied among animals depending on the recording conditions, we normalized the nerve activity by a 1-min averaged value during the baseline condition before applying stimulation. The minimal inter-burst activity of the nerve signal was treated as the zero level. To examine changes in AP, HR, CSNA, and RSNA, we used 10-s averaged data. The data were analyzed using repeated-measures one-way analysis of variance (ANOVA) followed by Dunnett's test (Glantz, 2002). The first data point of the baseline condition was treated as the control. To analyze the correlation between changes in AP and CSNA or RSNA, that between changes in AP and changes in HR, and that between CSNA and RSNA, we performed a linear regression analysis between the two variables (Glantz, 2002). To analyze the correlation between changes in HR and CSNA or RSNA, we first fit the relationship to the following equation using a nonlinear least square fitting (a downhill simplex method) (Nelder and Mead, 1965).

$$y = slope \times \log_{10}(offset + x) + intercept$$

where x and y represent changes in HR and sympathetic nerve activity, respectively. After determining the optimal offset value for x, an ordinary linear regression analysis was performed between [$\log_{10}$ (offset+x)] and y to examine the significance of the slope. In all of the regression analyses, the correlation was considered significant when the slope was significantly different from zero. We used paired-t test

to examine the difference between the CSNA and RSNA during the time period of maximum AP elevation induced by phenylephrine in Protocol 4. To examine the difference in the initial HR response to 10-Hz EA between Protocols 1 and 3, we used unpaired-t test because the number of trials was different between Protocols 1 and 3. The differences were considered significant at P<0.05.

3. Results

Typical recordings of 10-Hz EA obtained from two different cats are shown in Fig. 1. Horizontal arrows above the top panels indicate the period of EA. In one animal (Fig. 1A), AP was decreased by EA. HR decreased initially but increased from approximately 20 s after the onset of EA. As can be seen in the 2-s moving averaged signal (m-CSNA), CSNA exhibited changes similar to HR, i.e., it decreased at the onset of EA but gradually increased above the baseline level during the later portion of 1-min EA. RSNA and its 2-s moving averaged signal (m-RSNA) decreased at the onset of EA and gradually returned toward the baseline level. In another animal (Fig. 1B), both AP and HR were decreased by EA. Both CSNA and RSNA were also suppressed during EA, but the magnitude of suppression was greater in RSNA than in CSNA. Among the 5 animals, three showed the former type of AP and HR responses and remaining two showed the latter type. The type of AP and HR responses was consistent in each animal, i.e., the observed difference depended on the animal rather than the trial.

Fig. 2A summarizes changes in AP, HR, CSNA, and RSNA in response to 10-Hz EA. We performed EA trials in the left and right hind limbs in each animal and pooled data for 10 trials from 5 animals because there did not appear to be significant laterality in the effects of EA. The thick line on the abscissa in each panel indicates the period of EA. Baseline AP and HR values were 101 ±17 mmHg and 161 ±24 beats/min, respectively. AP was significantly decreased by EA and the decrease lasted over 1 min after
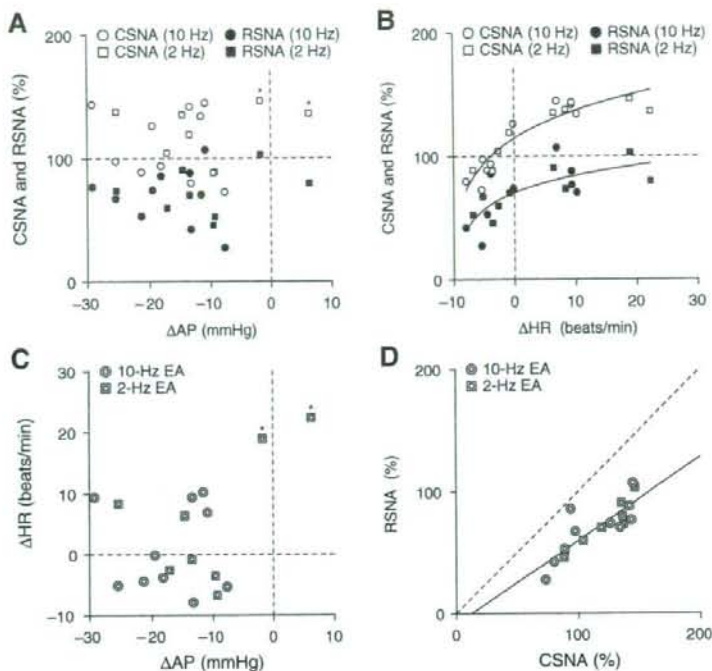
Fig. 3. Scatter plots of data obtained from the last 10 s of 1-min electroacupuncture (EA). A: Percent values of cardiac sympathetic nerve activity (CSNA) and renal sympathetic nerve activity (RSNA) plotted against changes in arterial pressure (ΔAP). Open and closed circles indicate CSNA and RSNA during 10-Hz EA, respectively. Open and closed squares indicate CSNA and RSNA during 2-Hz EA, respectively. Open squares with asterisks indicate data points where CSNA increased during EA even when AP did not decrease significantly or even increased. There was no significant relationship between changes in AP and CSNA ($r^2=0.0025$, $P=0.84$) or RSNA ($r^2=0.0039$, $P=0.81$). B: CSNA and RSNA plotted against changes in heart rate (ΔHR). Positive curvilinear relationships were observed between ΔHR and CSNA [CSNA$=83.0\times\log_{10}(11.5+\Delta$HR$)+26.7$, $r^2=0.86$, $P<0.01$] and between ΔHR and RSNA [RSNA$=46.6\times\log_{10}(10.1+\Delta$HR$)+23.6$, $r^2=0.56$, $P<0.01$]. C: Scatter plots of ΔHR versus ΔAP during 10-Hz EA (double circles) and 2-Hz EA (double squares). Except for the two data points with asterisks, there was no apparent relationship between changes in AP and those in HR ($r^2=0.17$, $P=0.094$ when the points with asterisk were included; $r^2=0.048$, $P=0.41$ when the points with asterisk were excluded). D: Scatter plots of RSNA versus CSNA during 10-Hz EA (double circles) and 2-Hz EA (double squares). There was a quasi-linear relationship between RSNA and CSNA (RSNA$=0.69\times$CSNA-8.8, $r^2=0.71$, $P<0.01$). The dashed line indicates the line of identity.

the cessation of EA. HR was significantly decreased in the first 20 s of EA but returned to the baseline level thereafter while EA continued. There was large variance in the CSNA response to EA among animals. Only the increase in CSNA after the cessation of EA was statistically significant. In contrast, RSNA was significantly decreased by EA during the entire period of EA.

Fig. 2B summarizes changes in AP, HR, CSNA, and RSNA in response to 2-Hz EA. We pooled data for 8 trials from 4 animals (left and right trials in each animal). Baseline AP and HR values were 98±17 mmHg and 151±20 beats/min, respectively. AP was decreased by EA, but the decrease was smaller and the duration of post-EA hypotension shorter than those observed in 10-Hz EA. HR increased with large variance during EA, and the increase was statistically significant after the cessation of EA. CSNA increased during the last 30 s of EA and remained increased for approximately 10 s after the cessation of EA. RSNA was decreased by EA during the period of EA, but the decrease appeared to be smaller than that observed with 10-Hz EA.

Fig. 3 illustrates scatter plots of data obtained during the last 10 s of EA. Because changes in AP nearly reached the steady state during the last 10 s of EA (Fig. 2A and B), we focused on these data. Open and closed circles in Fig. 3A and B indicates CSNA and RSNA data obtained from 10-Hz EA, respectively. Open and closed squares indicate CSNA and RSNA data obtained from 2-Hz EA, respectively. There was no apparent relationship between changes in AP and CSNA ($r^2=0.0025$, $P=0.84$) or RSNA ($r^2=0.0039$, $P=0.81$) by a linear regression analysis (Fig. 3A). In contrast, a positive curvilinear relationship was observed between changes in HR and CSNA [CSNA$=83.0\times\log_{10}(11.5+\Delta$HR$)+26.7$, $r^2=0.86$, $P<0.01$] or RSNA

[RSNA$=46.6\times\log_{10}(10.1+\Delta$HR$)+23.6$, $r^2=0.56$, $P<0.01$] (Fig. 3B). Double circles and squares in Fig. 3C and D indicate data obtained from 10-Hz EA and 2-Hz EA, respectively. In Fig. 3C, the two data points with asterisks indicate that 2-Hz EA increased HR by approximately 20 beats/min when changes in AP were close to zero or positive. However, except for the two data points, there was no apparent relationship between changes in AP and changes in HR ($r^2=0.17$, $P=0.094$ when the points with asterisk were included; $r^2=0.048$, $P=0.41$ when the points with asterisk were excluded). As indicated by Fig. 3A and B, the RSNA values were lower than the corresponding CSNA data (Fig. 3D), though CSNA and RSNA were both normalized to 100% during the baseline condition. A linear regression analysis revealed a significant positive correlation between CSNA and RSNA during the last 10 s of EA (RSNA$=0.69\times$CSNA-8.8, $r^2=0.71$, $P<0.01$).

As shown in Fig. 4A, there were no significant changes in AP, HR, CSNA, or RSNA during stimulation applied to a control point in the front of the right thigh. Baseline AP and HR values were 92±15 mmHg and 158±16 beats/min, respectively.

After sinoaortic denervation and vagotomy, baseline AP and HR values were 120±25 mmHg and 184±19 beats/min, respectively. As shown in Fig. 4B, 10-Hz EA decreased AP by approximately 30 mmHg. AP returned gradually to the pre-EA value after the cessation of EA. HR decreased slightly from 20 to 30 s and returned to the pre-EA baseline value thereafter. CSNA decreased only at the onset of EA. After the cessation of EA, CSNA exhibited a slight increase for approximately 20 s. RSNA decreased at the onset of EA. Although the magnitude of RSNA decrease became smaller with time, RSNA remained decreased during the period of EA.
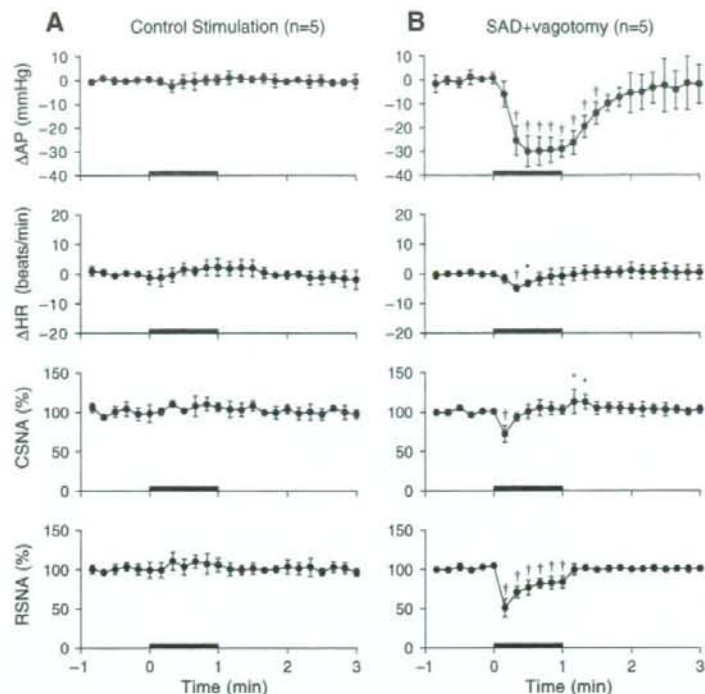
Fig. 4. Changes in arterial pressure (ΔAP), changes in heart rate (ΔHR), percent values of cardiac sympathetic nerve activity (CSNA), and percent values of renal sympathetic nerve activity (RSNA) during electrical stimulation at a nonspecific control point (A) and 10-Hz electroacupuncture (EA) after sinoaortic denervation (SAD) and vagotomy (B) averaged for all trials. Values are the mean ± SD. *P<0.05 and †P<0.01 from the first data point during pre-EA baseline period.

Fig. 5A depicts changes in AP, HR, CSNA, and RSNA induced by intravenous bolus injection of phenylephrine (5 µg/kg). The data were obtained before sinoaortic denervation and vagotomy. Baseline AP and HR values were 98±24 mmHg and 163±30 beats/min, respectively. As expected, phenylephrine increased AP but decreased HR. Both CSNA and RSNA were decreased by phenylephrine injection. The suppression of CSNA persisted longer than that of RSNA. There was no significant correlation between CSNA and RSNA during the baseline condition immediately before the administration of phenylephrine (Fig. 5B, white circles, r^2=0.32, P=0.32). When CSNA and RSNA were compared during the time period of phenylephrine-induced maximum AP elevation, there was no significant correlation either (Fig. 5B, filled circles, r^2=0.0003, P=0.98).

4. Discussion

We have demonstrated that CSNA and RSNA responded differentially to EA applied to a hind limb in pentobarbital-anesthetized cats. Although the CSNA and RSNA responses were discordant, we found that CSNA and RSNA attained a new linear relationship during the last 10 s of EA (Fig. 3D), regardless of the stimulus frequency of EA.

4.1. Effects of EA on CSNA and RSNA

The neural mechanisms underlying hemodynamic responses to acupuncture are not fully understood. Recently, Uchida et al. (2007) demonstrated that manual acupuncture-like stimulation of a hind limb decreased CSNA and HR in pentobarbital-anesthetized rats. Their results complement the study by Ohsawa et al. (1995) showing that manual acupuncture-like stimulation decreased RSNA and AP. Although these results suggest that manual acupuncture-like stimulation causes systemic sympathoinhibition, we noted that HR did not necessarily de-

crease even when EA produced hypotensive effects in pentobarbital-anesthetized cats (Figs. 1A and 2A and B). Simultaneous recordings of CSNA and RSNA in the present study clearly supported the hypothesis that EA evoked regional differences among sympathetic nerve activities. Fig. 1A is a typical case in which CSNA increased without an associated increase in RSNA during the later portion of EA. In Protocol 2, no significant changes were observed (Fig. 4A), suggesting that hemodynamic and sympathetic nerve activity responses observed in Protocol 1 were not nonspecific responses to electrical stimulation. This does not mean, however, the point below the knee joint just lateral to the tibia (corresponding to an ST36 acupoint in humans) is the only specific point to produce cardiovascular responses. For instance, EA at the forelimb (corresponding to a PC6 acupoint in humans) exerts the cardiovascular effects in rats (Lujan et al., 2007).

Averaged data for 10-Hz EA (Fig. 2A) revealed a discrepancy between the CSNA and RSNA responses to EA. Both sympathoinhibition and sympathoexcitation appear to have occurred in CSNA during EA. We suspected that strong electrical stimulation might have caused nociceptive sympathoexcitatory responses in CSNA. However, reducing the stimulus frequency from 10 to 2 Hz resulted in a more pronounced excitatory response in CSNA during the later period of 1-min EA (Fig. 2B), suggesting that the increase in CSNA during EA was not a nociceptive response. Another factor that should be taken into account is effects of anesthesia. Matsukawa et al. (Matsukawa et al., 1993) demonstrated that sympathoinhibition induced by acute intravenous pentobarbital administration was larger and lasted longer in the case of CSNA than in that of RSNA in cats. The sympathoinhibitory response to EA may be easily observed when the baseline sympathetic tone is high. Because baseline sympathetic tone was probably lower in CSNA than in RSNA due to the pentobarbital anesthesia, the sympathoinhibitory response in CSNA might have been masked or hard to observe.
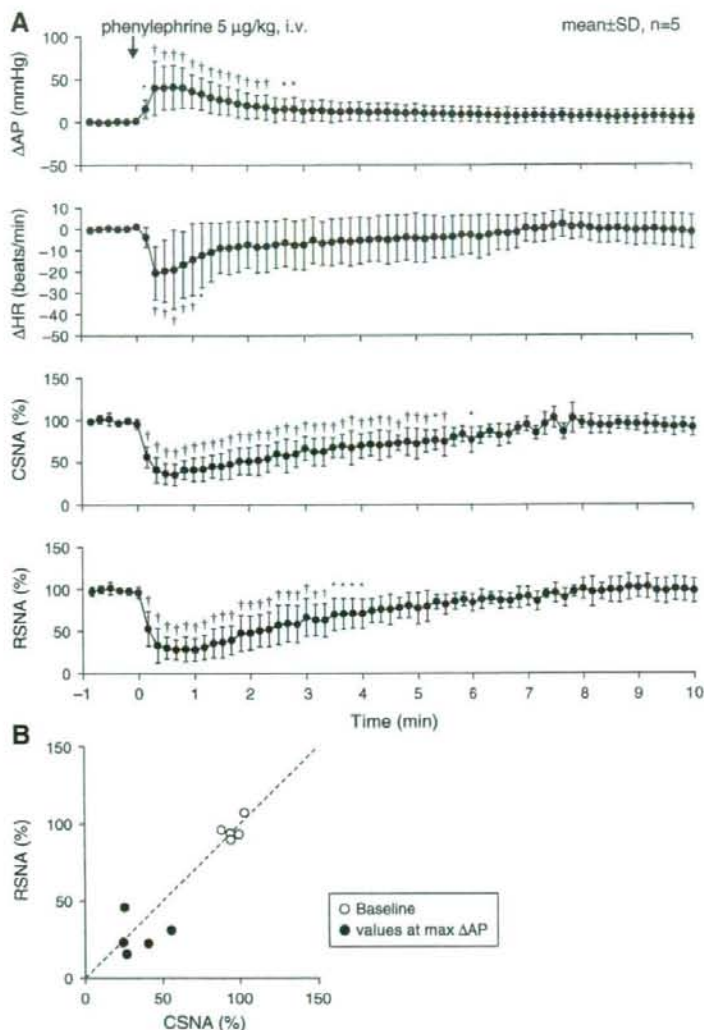
Fig. 5. A: Changes in arterial pressure (ΔAP), changes in heart rate (ΔHR), percent values of cardiac sympathetic nerve activity (CSNA), and percent values of renal sympathetic nerve activity (RSNA) during intravenous bolus injection of phenylephrine (5 µg/kg). Values are the mean±SD. *P<0.05 and †P<0.01 from the first data point during the baseline period. B: Scatter plots between CSNA and RSNA during the baseline condition immediately before the administration of phenylephrine (white circles) and those during the time period of phenylephrine-induced maximum AP elevation (filled circles). There was no significant correlation between CSNA and RSNA. The dashed line indicates the line of identity.

Although we measured left CSNA near the ventral ansa of the left stellate ganglion, there are several connections between the vagal and sympathetic nerves to form the cardiopulmonary nerves (Armour and Hopkins, 1984). Because we did not cut the vagi at the neck in Protocols 1 and 2, possibility of vagal contamination in the CSNA recording cannot be ruled out. However, because phenylephrine-induced hypertension that can increase vagal efferent activity (Kawada et al., 2001) attenuated CSNA to a similar degree to RSNA during the time period of maximum AP elevation (38.5±13.4% vs. 28.6±10.5%, P=0.32 by paired-t test, Fig. 5A), the effect of vagal contamination might have been a limited one.

4.2. Mechanistic considerations

In the present experimental settings, CSNA and RSNA exhibited decreasing responses to arterial baroreflex activation as demonstrated in previous studies (Fig. 5) (Minisi et al., 1989; Ninomiya et al., 1971),

confirming that what we measured as CSNA and RSNA represented efferent sympathetic nerve activities. Because EA caused hypotension, it could exert sympathoexcitatory effects through the arterial baroreflex in Protocol 1. If the baroreflex-mediated sympathoexcitatory effect is stronger for CSNA than for RSNA, this may account for the discrepancy between the CSNA and RSNA responses. However, in some trials, CSNA was increased even when AP did not decrease sizably or was even increased (Fig. 3A, open squares with asterisks), suggesting that the baroreflex-medicated sympathoexcitatory effect cannot explain the increase in CSNA. Actually, the discrepancy between the CSNA and RSNA responses to 10-Hz EA persisted after sinoaortic denervation and vagotomy (Fig. 4B). Therefore, CSNA might have been activated in the later period of EA via mechanisms other than baroreflexes. This interpretation is in line with the conclusion by Sato et al. (1981) that variable changes in HR in response to somatic afferent stimulation were not an indirect consequence of preceding changes in blood pressure.

Although electrical stimulation of groups I and II muscle nerves of fore and hind limbs was not effective in changing HR (McCloskey and Mitchell, 1972; Sato et al., 1981), additional stimulation of group III nerves induced either tachycardia or bradycardia in anesthetized cats (Khayutin et al., 1986; Sato et al., 1981). Further, additional stimulation of group IV muscle nerves of a hind limb always produced tachycardia (Johansson, 1962; Tibes, 1977), with an optimal frequency between 6 and 15 Hz (Sato et al., 1981). In the present study, activation of group IV muscle nerves unlikely explain the tachycardiac response, since reducing the stimulus frequency from 10 to 2 Hz did not attenuate the tachycardiac response. Although Sato et al. (1981) concluded that whether group III muscle afferent stimulation induces tachycardia or bradycardia was difficult to predict, we found that there was a quasi-linear relationship between RSNA and CSNA during the last 10 s of 1-min EA, regardless of the stimulus frequency (Fig. 3D). When the sympathoinhibition assessed by RSNA was strong enough, CSNA decreased during EA. When the sympathoinhibition assessed by RSNA was weak, CSNA increased.

4.3. Limitations

Several limitations need to be addressed. First, we performed experiments under pentobarbital anesthesia. Our results might have differed had we used different anesthesia or performed the experiments in conscious animals. However, Sato et al. (1981) used chloralose and urethane anesthesia and reported divergence of HR responses induced by group III muscle fiber afferent stimulation. Therefore, the differences between CSNA and RSNA might not be explained by type of anesthesia alone.

Second, we measured only CSNA and RSNA. Changes in AP did not correlate with CSNA or RSNA (Fig. 3A), suggesting that the AP response to EA was not explained by changes in CSNA or RSNA. The abdominal vascular bed plays a significant role in the arterial blood pressure control (Rowell, 1974). Further studies such as that recording splanchnic nerve activity are needed to elucidate the total picture of the sympathetic mechanism for the AP response to EA.

Third, we did not perform vagotomy independently of sinoaortic denervation. Accordingly, the contribution of vagal nerve activity to the HR response was not identified. Comparing Figs. 2A and 4B, the initial drop in HR was much clearer before sinoaortic denervation and vagotomy (P = 0.025 during the first 10 s after EA initiation by unpaired-t test) despite the similar profile of CSNA response to EA. Therefore, the vagal nerve activity might have contributed to the initial drop in HR in response to EA.

4.4. Conclusion

We demonstrated that EA evoked regional differences between CSNA and RSNA in pentobarbital-anesthetized cats. The differences persisted after sinoaortic denervation and vagotomy, suggesting the baroreflex-mediated sympathoexcitatory mechanisms alone cannot explain the discrepancy between CSNA and RSNA responses during EA. Although the responses were discordant, there was a linear relationship that persisted between CSNA and RSNA during the last 10 s of 1-min EA, suggesting that EA changes the relationship between CSNA and RSNA.

Acknowledgments

References

Armour, J.A., Hopkins, D.A., 1984. Anatomy of the extrinsic efferent autonomic nerves and ganglia innervating the mammalian heart. In: Randall, W.C. (Ed.), Nervous Control of Cardiovascular Function. Oxford Univ. Press, New York, pp. 20–45.
DiBona, G.F., 2005. Physiology in perspective: the wisdom of the body. Neural control of the kidney. Am. J. Physiol., Regul. Integr. Comp. Physiol. 289 (3), R633–641.
Glantz, S.A., 2002. Primer of Biostatistics, 5th ed. McGraw-Hill, New York.
Johansson, B., 1962. Circulatory responses to stimulation of somatic afferents with special reference to depressor effects from muscle nerves. Acta Physiol. Scand., Suppl. 198, 1–91.
Kawada, T., Yamazaki, T., Akiyama, T., Shishido, T., Inagaki, M., Uemura, K., Miyamoto, T., Sugimachi, M., Takaki, H., Sunagawa, K., 2001. In vivo assessment of acetylcholine-releasing function at cardiac vagal nerve terminals. Am. J. Physiol. Heart Circ. Physiol. 281 (1), H139–145.
Kawada, T., Uemura, K., Kashihara, K., Jin, Y., Li, M., Zheng, C., Sugimachi, M., Sunagawa, K., 2003. Uniformity in dynamic baroreflex regulation of left and right cardiac sympathetic nerve activities. Am. J. Physiol., Regul. Integr. Comp. Physiol. 284 (6), R1506–1512.
Khayutin, V.M., Lukoshkova, E.V., Gailans, J.B., 1986. Somatic depressor reflexes: results of specific 'depressor' afferents' excitation or an epiphenomenon of general anesthesia and certain decerebrations? J. Auton. Nerv. Syst. 16 (1), 35–60.
Kimura, A., Sato, A., 1997. Somatic regulation of autonomic functions in anesthetized animals—neural mechanisms of physical therapy including acupuncture. Jpn. J. Vet. Res. 45 (3), 137–145.
Kline, R.L., Yeung, K.Y., Calaresu, F.R., 1978. Role of somatic nerves in the cardiovascular responses to stimulation of an acupuncture point in anesthetized rabbits. Exp. Neurol. 61 (3), 561–570.
Kobayashi, S., Noguchi, E., Ohsawa, H., Sato, Y., Nishijo, K., 1998. Experimental research on the reflex decrease of heart rate elicited by acupuncture stimulation in anesthetized rats (in Japanese). Jpn. Acupunct. Moxib. 48, 120–129.
Ku, Y.H., Zou, C.J., 1993. Tinggong (SI 19), a novel acupoint for 2 Hz electroacupuncture-induced depressor response. Acupunct. Electrother. Res. 18 (2), 89–96.
Lee, H.S., Kim, J.Y., 1994. Effects of acupuncture on blood pressure and plasma renin activity in two-kidney one clip Goldblatt hypertensive rats. Am. J. Chin. Med. 22 (3–4), 215–219.
Lin, M.C., Nahin, R., Gershwin, M.E., Longhurst, J.C., Wu, K.K., 2001. State of complementary and alternative medicine in cardiovascular, lung, and blood research: executive summary of a workshop. Circulation 103 (16), 2038–2041.
Lujan, H.L., Kramer, V.J., DiCarlo, S.E., 2007. Electroacupuncture decreases the susceptibility to ventricular tachycardia in conscious rats by reducing cardiac metabolic demand. Am. J. Physiol. Heart Circ. Physiol. 292 (5), H2550–H2555.
Matsukawa, K., Ninomiya, I., Nishiura, N., 1993. Effects of anesthesia on cardiac and renal sympathetic nerve activities and plasma catecholamines. Am. J. Physiol. 265 (4 Pt 2), R792–R797.
McCloskey, D.I., Mitchell, J.H., 1972. Reflex cardiovascular and respiratory responses originating in exercising muscle. J. Physiol. 224 (1), 173–186.
Minisi, A.J., Dibner-Dunlap, M., Thames, M.D., 1989. Vagal cardiopulmonary baroreflex activation during phenylephrine infusion. Am. J. Physiol. 257 (5 Pt 2), R1147–R1153.
Nelder, J.A., Mead, R., 1965. A simplex method for function minimization. Comput. J. 7, 308–313.
Ninomiya, I., Nisimaru, N., Irisawa, H., 1971. Sympathetic nerve activity to the spleen, kidney, and heart in response to baroceptor input. Am. J. Physiol. 221 (5), 1346–1351.
Ohsawa, H., Okada, K., Nishijo, K., Sato, Y., 1995. Neural mechanism of depressor responses of arterial pressure elicited by acupuncture-like stimulation to a hindlimb in anesthetized rats. J. Auton. Nerv. Syst. 51 (1), 27–35.
Rowell, L.B., 1974. Human cardiovascular adjustments to exercise and thermal stress. Physiol. Rev. 54 (1), 75–159.
Sato, A., Sato, Y., Schmidt, R.F., 1981. Heart rate changes reflecting modifications of efferent cardiac sympathetic outflow by cutaneous and muscle afferent volleys. J. Auton. Nerv. Syst. 4 (3), 231–247.
Sato, A., Sato, Y., Suzuki, A., Uchida, S., 1994. Reflex modulation of gastric and vesical function by acupuncture-like stimulation in anesthetized rats. Biomed. Res. 15, 59–65.
Sato, A., Sato, Y., Uchida, S., 2002. Reflex modulation of visceral functions by acupuncture-like stimulation in anesthetized rats. Int. Congr. Ser. 1238, 111–123.
Tibes, U., 1977. Reflex inputs to the cardiovascular and respiratory centers from dynamically working canine muscles. Some evidence for involvement of group III or IV nerve fibers. Circ. Res. 41 (3), 332–341.
Uchida, S., Shimura, M., Ohsawa, H., Suzuki, A., 2007. Neural mechanism of bradycardic responses elicited by acupuncture-like stimulation to a hind limb in anesthetized rats. J. Physiol. Sci. 57 (6), 377–382.
Yasunaga, K., Nosaka, S., 1979. Cardiac sympathetic nerves in rats: anatomical and functional features. Jpn. J. Physiol. 29 (6), 691–705.
Zhou, W., Fu, L.W., Tjen, A.L.S.C., Li, P., Longhurst, J.C., 2005. Afferent mechanisms underlying stimulation modality-related modulation of acupuncture-related cardiovascular responses. J. Appl. Physiol. 98 (3), 872–880.

Accentuated Antagonism in Vagal Heart Rate Control Mediated through Muscarinic Potassium Channels

Masaki MIZUNO[1], Atsunori KAMIYA[1], Toru KAWADA[1], Tadayoshi MIYAMOTO[2],
Shuji SHIMIZU[1,3], Toshiaki SHISHIDO[1], and Masaru SUGIMACHI[1]

[1]Department of Cardiovascular Dynamics, Advanced Medical Engineering Center, National Cardiovascular Center Research
Institute, Osaka, Japan; [2]Department of Physical Therapy, Faculty of Health Sciences, Morinomiya University of Medical Sciences,
Osaka, Japan; and [3]Japan Association for the Advancement of Medical Equipment, Tokyo, Japan

Abstract: Although muscarinic K^+ (K_{ACh}) channels contribute to a rapid heart rate (HR) response to vagal stimulation, whether background sympathetic tone affects the HR control via the K_{ACh} channels remains to be elucidated. In seven anesthetized rabbits with sinoaortic denervation and vagotomy, we estimated the dynamic transfer function of the HR response by using random binary vagal stimulation (0–10 Hz). Tertiapin, a selective K_{ACh} channel blocker, decreased the dynamic gain (to 2.3 ± 0.9 beats·min^{-1}·Hz^{-1}, from 4.6 ± 1.1, $P < 0.01$, mean $\pm$ SD) and the corner frequency (to 0.05 ± 0.01 Hz, from 0.26 ± 0.04, $P < 0.01$). Under 5 Hz tonic cardiac sympathetic stimulation (CSS), tertiapin decreased the dynamic gain (to 3.6 ± 1.0 beats·min^{-1}·Hz^{-1}, from 7.3 ± 1.1, $P < 0.01$) and the corner frequency (to 0.06 ± 0.02 Hz, from 0.23 ± 0.06, $P < 0.01$). Two-way analysis of variance indicated significant interaction between the tertiapin and CSS effects on the dynamic gain. In contrast, no significant interactions were observed between the tertiapin and CSS effects on the corner frequency and the lag time. In conclusion, although a cyclic AMP-dependent mechanism has been well established, an accentuated antagonism also occurred in the direct effect of ACh via the K_{ACh} channels. The rapidity of the HR response obtained by the K_{ACh} channel pathway was robust during the accentuated antagonism.

Key words: systems analysis, transfer function, muscarinic receptor, sympathovagal interaction, accentuated antagonism, rabbit.

Vagal control of heart rate (HR) is mediated by ACh, which activates M_2 muscarinic receptors and heterotrimeric G_i and/or G_o proteins in cardiac myocytes [1]. The actions of ACh are determined by the G_i protein subunits. The α subunits of the G_i proteins inhibit adenylyl cyclase and decrease HR by counteracting the sympathetic effects [2], whereas $\beta\gamma$ subunits activate inwardly rectifying muscarinic K^+ (K_{ACh}) channels and decrease HR by hyperpolarizing the maximum diastolic potential in the sinus node cells [3–5]. Hereafter in the present paper, we refer to the former action as the indirect action of ACh and the latter action as the direct action of ACh. In a previous paper, we demonstrated that a selective K_{ACh} channel blocker tertiapin decreased and slowed the HR response to dynamic vagal stimulation, suggesting that the K_{ACh} channels contribute to a rapid HR response to vagal stimulation [6]. However, whether background sympathetic tone affects HR control via the K_{ACh} channels remains to be elucidated. Because pathophysiological conditions such as chronic heart failure [7], hypertension [8], and obesity [9] often display increased sympathetic nerve

activity, it would be important to quantify the effects of background sympathetic tone on the HR response via the K_{ACh} channels for a better understanding of the vagal HR control in such disease states.

We made two hypotheses regarding sympathetic effects on vagal HR control via the K_{ACh} channels. With respect to the speed of HR regulation, the indirect action of ACh relies on slower changes in intracellular cyclic AMP levels [10, 11]. In contrast, the direct action of ACh utilizes the faster membrane-delimited mechanisms of K_{ACh} channels and is believed to be independent of sympathetic control [12]. Accordingly, we first hypothesized that background sympathetic tone would not affect the *rapidity* of HR control provided by the K_{ACh} channel pathway. With respect to the magnitude of HR regulation, complex sympathovagal interactions can occur in autonomic HR control. Levy [13] termed the phenomenon that background sympathetic tone augmented vagal HR control "an accentuated antagonism." Kawada *et al.* [14] demonstrated that sympathovagal interaction bidirectionally increased the dynamic gain of HR control, even

though the sympathetic and vagal systems affected mean HR antagonistically. Therefore we then hypothesized that background sympathetic tone would augment the *magnitude* of the HR response to vagal stimulation via K_{ACh} channels.

To test the above-mentioned hypotheses, we examined the dynamic and static transfer characteristics of the HR response to vagal stimulation using a selective K_{ACh} channel blocker tertiapin and concomitant cardiac sympathetic stimulation (CSS). Observation of significant interaction between tertiapin and CSS effects might allow us to deduce that background sympathetic tone influences the direct action of ACh via K_{ACh} channels.

MATERIALS AND METHODS

Surgical preparations. Animal care was consistent with "Guiding Principles for the Care and Use of Animals in the Field of Physiological Sciences" of the Physiological Society of Japan. All protocols were reviewed and approved by the Animal Subjects Committee of the National Cardiovascular Center. Seven Japanese white rabbits (2.7–3.2 kg body wt) were anesthetized using a mixture of urethane (250 mg/ml) and α-chloralose (40 mg/ml): an initial bolus dose of 2 ml/kg and a maintenance dose of 0.5 ml·kg^{-1}·h^{-1}. The rabbits were intubated and mechanically ventilated with oxygen-enriched room air. Arterial pressure (AP) was measured by a micromanometer (SPC-330A, Millar Instruments, Houston, TX, USA) inserted into the right femoral artery and advanced to the thoracic aorta. HR was measured with a cardiotachometer (model N4778, San-ei, Tokyo, Japan). A double-lumen catheter was introduced into the right femoral vein for continuous anesthetic and drug administration. Sinoaortic denervation was performed bilaterally to minimize changes in sympathetic efferent nerve activity via arterial baroreflexes. The main branches of the cardiac postganglionic sympathetic nerves were sectioned bilaterally through a midline thoracotomy. A pair of bipolar platinum electrodes was attached to the cardiac end of the sectioned right inferior cardiac sympathetic postganglionic nerve for tonic cardiac sympathetic nerve stimulation [15]. The vagi were sectioned bilaterally at the neck. Another pair of bipolar electrodes was attached to the cardiac end of the sectioned right vagus for vagal stimulation. Immersion of the stimulation electrodes and nerves in a mixture of white petroleum jelly (Vaseline) and liquid paraffin prevented the nerves from drying and also provided insulation. Body temperature was maintained at 38°C with a heating pad throughout the experiment.

Experimental protocols. The pulse duration of nerve stimulation was set at 2 ms. The stimulation amplitude of the right vagus was first adjusted in each animal to yield an HR decrease of ~50 beats/min at 10 Hz constant stimulation (1.6–6.0 V, 3.2 ± 1.7 V, mean ± SD) and fixed.

The stimulation amplitude of the right cardiac sympathetic nerve was also adjusted in each animal to yield an HR increase of ~50 beats/min at 5 Hz constant stimulation (1.5–3.5 V, 2.2 ± 0.8 V) and fixed. Approximately 1 h elapsed after the completion of surgical preparation until stable hemodynamics were attained.

Dynamic protocol (*n* = 7). For an estimation of the dynamic transfer characteristics from vagal stimulation to the HR response, the right vagus was stimulated by a frequency-modulated pulse train for 10 min. The stimulation frequency was switched every 500 ms at either 0 or 10 Hz according to a binary white-noise signal. The power spectrum of the stimulation signal was reasonably constant up to 1 Hz. The transfer function was estimated up to 1 Hz because the reliability of estimation decreased as a result of the diminution of input power above this frequency. The selected frequency range spanned the frequency range of physiological interest sufficiently with respect to the dynamic vagal control of HR in rabbits.

Static protocol (*n* = 5). For an estimation of the static transfer characteristics between vagal stimulation and HR response, stepwise vagal stimulation was performed. Vagal stimulation frequency was increased to 20 Hz, from 5, in 5 Hz increments. Each frequency step was maintained for 60 s.

Pharmacological intervention. We used a selective K_{ACh} channel blocker tertiapin (Peptide Institute, Inc., Osaka, Japan) to block the direct action of ACh in vagal HR control. The dynamic and static characteristics of the heart rate response to vagal stimulation were estimated with and without CSS. After the tertiapin-free data were obtained, a bolus dose (30 nmol/kg iv) of tertiapin was administered. Fifteen min thereafter, the dynamic and static characteristics were estimated again, with and without CSS. The tertiapin-free data were obtained first in all animals because the long-lasting (>2 h) effects of tertiapin did not permit the acquisition of tertiapin-free data after the tertiapin administration. The order of dynamic and static protocols and the order of CSS application were randomly assigned in different animals. An intervening interval of more than 5 min was allowed between the dynamic and static protocols so that AP and HR returned their prestimulation values.

Data analysis. A 12-bit analog-to-digital converter was used to digitize the AP and HR recordings at 200 Hz, and the data were stored on the hard disk of a dedicated laboratory computer system. The dynamic transfer function from binary white-noise vagal stimulation to the HR response was estimated as follows. Input-output data pairs of the vagal stimulation frequency and HR were resampled at 10 Hz; then data pairs were partitioned into eight 50%-overlapping segments, each consisting of 1,024 data points. For each segment, the linear trend was subtracted and a Hanning window applied. A fast Fourier transform was then performed to obtain the frequency

spectra for vagal stimulation $[N(f)]$ and HR $[HR(f)]$ [16]. Over the eight segments, the power of the vagal stimulation $[S_{NN}(f)]$, the power of the HR $[S_{HR\cdot HR}(f)]$, and the cross-power between these two signals $[S_{N\cdot HR}(f)]$ were ensemble averaged. Lastly, the transfer function $[H(f)]$ from vagal stimulation to the HR response was estimated as follows [17, 18].

$$[H(f)] = \frac{S_{N\cdot HR}(f)}{S_{NN}(f)} \tag{1}$$

In previous studies [6, 14] the transfer function from vagal stimulation to HR response approximated a first-order, low-pass filter with a lag time; therefore the estimated transfer function was parameterized using the following mathematical model.

$$H(f) = \frac{-K}{1 + \dfrac{f}{fc} j} e^{-2\Pi f j L} \tag{2}$$

where K represents the dynamic gain (or, to be more accurate, the steady-state gain, in beats·min^{-1}·Hz^{-1}), fc denotes the corner frequency (in Hz), L denotes the lag time (in s), and f and j represent frequency and imaginary unit, respectively. The negative sign in the numerator indicates the negative HR response to vagal stimulation. The steady-state gain indicates the asymptotic value of the relative amplitude of HR response to vagal nerve stimulation when the frequency of input modulation approaches zero. The corner frequency represents the frequency of input modulation at which gain decreases by 3 dB from the steady-state gain in the frequency domain. The corner frequency reflects the rapidity of the HR response to vagal stimulation; the higher the corner frequency, the faster the HR response. The dynamic gain, corner frequency, and lag time were estimated by means of an iterative nonlinear least-squares regression. The phase shift of the transfer function indicates, with respect to the input signal, a lag or lead in the output signal normalized by its corresponding frequency of input modulation.

To quantify the linear dependence of the HR response on vagal stimulation, the magnitude-squared coherence function $[Coh(f)]$ was estimated as follows [17, 18].

$$[Coh(f)] = \frac{|S_{N\cdot HR}(f)|^2}{S_{NN}(f) \cdot S_{HR\cdot HR}(f)} \tag{3}$$

Coherence values range from zero to unity. Unity coherence indicates perfect linear dependence between the input signals and output signals; in contrast, zero coherence indicates total independence between the two.

To facilitate the intuitive understanding of the system dynamic characteristics, we calculated the system step response of HR to 1 Hz nerve stimulation as follows. The system impulse response was derived from the inverse Fourier transform of $H(f)$. The system step response was then obtained from the time integral of the impulse response. The length of the step response was 51.2 s. We calculated the maximum step response by averaging the

last 10 s of the step response. The time constant of the step response was calculated from the corner frequency of the corresponding transfer function using the following relationship.

$$\text{Time constant} = \frac{1}{2 \cdot \Pi \cdot fc} \tag{4}$$

In this definition, the time constant is related inversely to the corner frequency without being influenced by the lag time.

The static transfer function from stepwise vagal stimulation to HR was estimated by averaging the HR data during the final 10 s of the 60 s stimulation at each stimulation step.

Statistical analysis. Values are mean ± SD. A two-way ANOVA, with drug and CSS as the main effects, was used to test the differences among parameters. $P < 0.05$ was considered significant.

RESULTS

Figure 1A shows recordings typical of the dynamic protocol. The top panels show HR under conditions of control (thin lines) and K_{ACh} channel blockade (thick lines), without (left) and with (right) CSS. The bottom panels show the binary white-noise signal used for vagal stimulation. Random vagal stimulation decreased HR intermittently. Tertiapin attenuated the HR variation in response to the dynamic vagal stimulation. CSS increased the mean level of HR and augmented HR variation in response to the dynamic vagal stimulation.

Figure 1B shows recordings typical of the static protocol. The top panels illustrate HR under conditions of control (thin lines) and K_{ACh} channel blockade (thick lines), without (left) and with (right) CSS. The bottom panels depict the vagal stimulation frequency. The stepwise vagal stimulation decreased HR in a stepwise manner. Tertiapin attenuated the bradycardic response to vagal stimulation regardless of CSS, which increased baseline HR and contributed to augment the response.

Dynamic protocol

The mean values of AP and HR before and during dynamic vagal stimulation are summarized in Table 1. This stimulation did not affect AP under any of the conditions, but it significantly decreased the mean HR except under the conditions of K_{ACh} channel blockade without CSS, which increased the mean HR ($P < 0.01$), but not the mean AP, both before and during vagal stimulation.

Figure 2A illustrates the dynamic transfer functions characterizing the vagal HR control averaged for all animals under conditions of control (thin lines) and K_{ACh} channel blockade (thick lines), without (left) and with (right) CSS. Gain plots, phase plots, and coherence functions are shown. Note that the frequency axes of these plots indicate the modulation frequency of the random
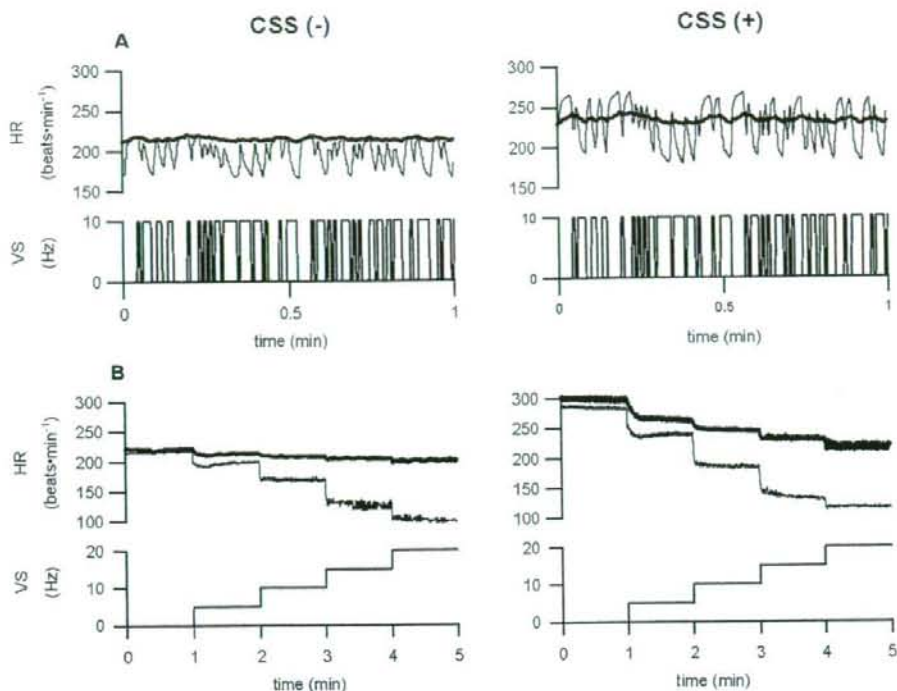
Fig. 1. A: Representative recordings of HR obtained utilizing binary white-noise vagal stimulation (top) and the corresponding vagal stimulation (VS; bottom) without (left) and with (right) CSS. Thin line, control; thick line, K_{ACh} channel blockade with tertiapin (30 nmol·kg⁻¹ iv). **B**: Representative recordings of HR obtained utilizing stepwise vagal stimulation (top) and the corresponding VS (bottom) without (left) and with (right) CSS, which increased the basal HR and the amplitude of HR variation in both binary white-noise and stepwise vagal stimulations. A K_{ACh} channel blockade attenuated the amplitude of HR variation and the speed of the response of HR to vagal stimulation regardless of CSS.

Table 1. Effects of tertiapin infusion and CSS on AP and HR before and during dynamic vagal stimulation.

	CSS (−)		CSS (+)		Comparison factors		
	Control	Tertiapin	Control	Tertiapin	Drug	CSS	Interaction
AP, mmHg							
Before stimulation	82.2 ± 16.8	76.7 ± 20.1	90.5 ± 13.8	81.8 ± 16.6	0.022	0.641	0.546
During stimulation	80.2 ± 18.4	76.6 ± 21.4	81.8 ± 14.8	75.9 ± 19.0	0.144	0.962	0.709
HR, beats·min⁻¹							
Before stimulation	247.8 ± 20.1	247.9 ± 30.8	312.2 ± 15.6	307.4 ± 20.9	0.521	<0.001	0.494
During stimulation	211.9 ± 17.5**	228.3 ± 23.4	244.3 ± 33.3**	248.1 ± 30.7**	0.026	<0.001	0.308

Values are means ± SD ($n = 7$). CSS, cardiac sympathetic stimulation; AP, arterial pressure; HR, heart rate. **$P < 0.01$ vs. corresponding values before stimulation. Tertiapin was infused at 30 nmol/kg iv.

input signal and not the vagal stimulation frequency itself. Table 2 summarizes parameters of the transfer function at 0.01, 0.1, 0.5, and 1 Hz and also those of the step response. Tertiapin attenuated the dynamic gain compared with the control conditions regardless of CSS. The phase approached −Π radians at the lowest frequency and lagged with increasing frequency under the control conditions. Tertiapin increased the phase delay in the

frequency range from 0.01 to 1 Hz. Coherence was near unity in the overall frequency range under the control conditions. A decrease in the coherence function from unity was noted >0.6 Hz under the condition of the K_{ACh} channel blockade, which was reversed by CSS.

Figure 2B shows the calculated step response of HR to vagal stimulation averaged for all animals under the conditions of control (thin lines) and K_{ACh} channel blockade
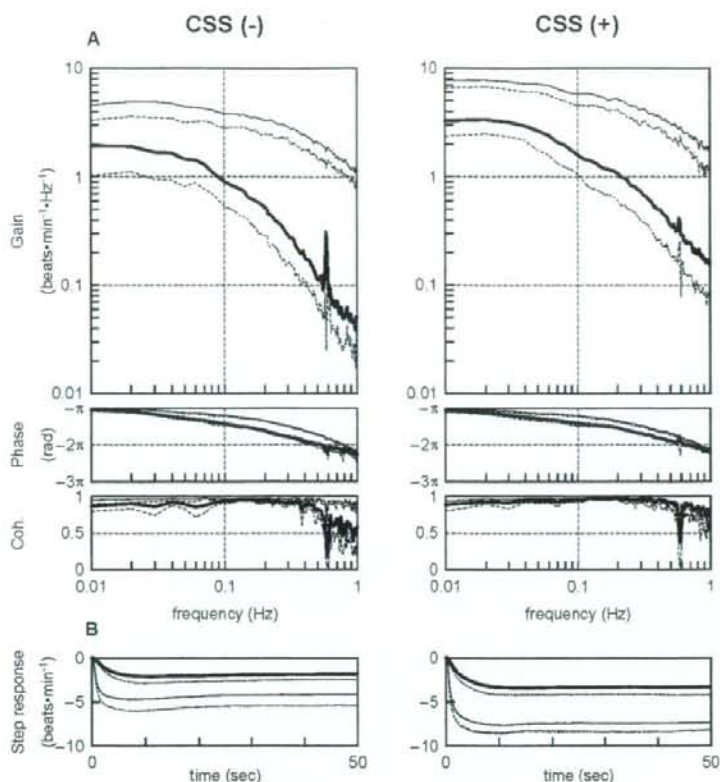
Fig. 2. A: Dynamic transfer function relating vagal stimulation to the HR responses averaged from all animals (pooled data; $n = 7$) without (left) and with (right) CSS. Solid lines, means; dashed lines, −SD. Thin line, control; thick line, a K_{ACh} channel blockade with tertiapin (30 nmol·kg^{-1} iv). Top: gains; middle: phase shifts; bottom: coherence (Coh) functions. Tertiapin decreased transfer gain and increased the phase shift with increasing frequency. Cardiac sympathetic stimulation increased transfer gain both under control conditions and under conditions of a K_{ACh} channel blockade without affecting the phase shift. B: Calculated step response to 1 Hz tonic vagal stimulation averaged from all animals (pooled data; $n = 7$) without (left) and with (right) CSS. Solid lines, means; dashed lines, −SD. Thin line, control; thick line, K_{ACh} channel blockade with tertiapin (30 nmol·kg^{-1} iv). The K_{ACh} channel blockade decreased the maximum step response and slowed the initial step response. CSS increased the maximum step response both under control conditions and under conditions of a K_{ACh} channel blockade without affecting the initial response (see Table 2).

Table 2. Effects of tertiapin infusion and CSS on parameters of the transfer function and step response.

	CSS (−)		CSS (+)		Comparison factors		
	Control	Tertiapin	Control	Tertiapin	Drug	CSS	Interaction
Gain, beats·min^{-1}·Hz^{-1}							
0.01 Hz	4.58 ± 1.26	2.21 ± 0.97	7.73 ± 1.15	3.28 ± 0.92	<0.001	0.001	0.007
0.1 Hz	3.81 ± 1.01	1.10 ± 0.43	5.82 ± 1.28	1.60 ± 0.54	<0.001	0.007	0.015
0.5 Hz	2.12 ± 0.64	0.16 ± 0.07	3.08 ± 0.82	0.36 ± 0.17	<0.001	0.013	0.081
1 Hz	1.09 ± 0.27	0.08 ± 0.03	1.73 ± 0.61	0.16 ± 0.08	<0.001	0.019	0.044
Phase, rad							
0.01 Hz	3.10 ± 0.04	2.99 ± 0.11	2.99 ± 0.11	2.92 ± 0.14	0.037	0.077	0.579
0.1 Hz	2.52 ± 0.08	1.78 ± 0.17	2.52 ± 0.11	1.83 ± 0.25	<0.001	0.757	0.719
0.5 Hz	0.91 ± 0.13	0.03 ± 0.27	0.90 ± 0.10	0.35 ± 0.10	<0.001	0.011	0.056
1 Hz	−0.56 ± 0.33	−0.81 ± 0.21	−0.41 ± 0.26	−0.64 ± 0.18	0.014	0.159	0.905
Coherence							
0.01 Hz	0.95 ± 0.05	0.87 ± 0.07	0.93 ± 0.04	0.89 ± 0.09	0.005	0.947	0.424
0.1 Hz	0.96 ± 0.03	0.94 ± 0.04	0.97 ± 0.01	0.95 ± 0.02	0.004	0.440	0.835
0.5 Hz	0.96 ± 0.02	0.83 ± 0.08	0.91 ± 0.08	0.93 ± 0.04	0.026	0.259	0.006
1 Hz	0.90 ± 0.07	0.59 ± 0.16	0.78 ± 0.15	0.79 ± 0.12	0.017	0.312	0.011
Maximum step response, beats·min^{-1}	−4.2 ± 1.2	−1.8 ± 0.6	−7.4 ± 0.9	−3.3 ± 0.9	<0.001	<0.001	0.005
Time constant, s	0.63 ± 0.09	3.34 ± 0.55	0.74 ± 0.18	3.18 ± 1.10	<0.001	0.913	0.560

Values are means ± SD ($n = 7$). CSS, cardiac sympathetic stimulation. Tertiapin was infused at 30 nmol/kg iv.

Table 3. Effects of tertiapin infusion and CSS on parameters of the transfer function relating dynamic vagal stimulation to HR.

	CSS (−)		CSS (+)		Comparison factors		
	Control	Tertiapin	Control	Tertiapin	Drug	CSS	Interaction
Dynamic gain, beats·min^{-1}·Hz^{-1}	4.6 ± 1.1	2.3 ± 0.9	7.3 ± 1.1	3.6 ± 1.0	<0.001	<0.001	0.037
Corner frequency, Hz	0.26 ± 0.04	0.05 ± 0.01	0.23 ± 0.06	0.06 ± 0.02	<0.001	0.439	0.1613
Lag time, s	0.38 ± 0.04	0.45 ± 0.04	0.34 ± 0.04	0.38 ± 0.03	<0.001	0.002	0.2776

Values are means ± SD ($n = 7$). CSS, cardiac sympathetic stimulation; HR, heart rate. Tertiapin was infused at 30 nmol/kg iv.

(thick lines), without (left) and with (right) CSS. Tertiapin slowed the transient response and attenuated the HR response to vagal stimulation in the time domain. CSS did not affect the time constant, though it augmented the maximum step response. A significant interaction was observed between the tertiapin and CSS effects in the maximum step response, but not in the time constant (Table 2).

The fitted parameters of the transfer functions are summarized in Table 3. Tertiapin significantly decreased the dynamic gain and the corner frequency and significantly increased the lag time. Conversely, CSS significantly increased the dynamic gain and significantly decreased the lag time. A significant interaction was observed between the tertiapin and CSS effects only in dynamic gain.

Static protocol

Figure 3A summarizes changes in HR in response to stepwise vagal stimulation without (left) and with (right) CSS, which increased basal HR obtained at 0 Hz vagal stimulation by approximately 50 beats·min^{-1}. Tertiapin significantly attenuated the bradycardic response to vagal stimulation regardless of CSS. The magnitude of attenuation (i.e., the difference between the open and closed symbols) became greater as the vagal stimulation frequency increased.

Figure 3B demonstrates the HR reduction obtained under four conditions at each frequency. To aid an intuitive understanding, the tertiapin condition is designated as D(−) in this panel because tertiapin blocked the direct action of ACh. S(+) indicates the presence of CSS. At 5 Hz vagal stimulation frequency, the direct action alone S(−)D(+) significantly augmented the HR reduction, as depicted by the diagonal hatch. CSS alone S(+)D(−) also significantly augmented the HR reduction, as depicted by the vertical hatch. The augmentation of the HR reduction obtained by S(+)D(+) exceeded the simple summation of the diagonal hatch and vertical hatch, suggesting that the effect of the direct action was enhanced by CSS (depicted in the solid rectangle). The positive interaction waned at 10 Hz vagal stimulation and disappeared at 15 and 20 Hz vagal stimulation. That is, the simple summation of the

diagonal hatch and vertical hatch largely explained the augmentation of the HR reduction attained by S(+)D(+) at 15 and 20 Hz vagal stimulation.

DISCUSSION

We have examined the effect of background sympathetic tone on the direct action of ACh through K_{ACh} channels by examining the dynamic and static transfer characteristics. The major findings in the present study are that the bradycardic response to vagal stimulation via the K_{ACh} channels was augmented by concomitant CSS, depending on vagal stimulation frequency. The rapidity of vagal HR control obtained by the K_{ACh} channels, however, was not affected by CSS. These findings support our hypotheses and demonstrated, for the first time to our knowledge, the existence of an accentuated antagonism in the direct action of ACh through the K_{ACh} channels.

Effect of CSS on the rapidity of vagal HR control via K_{ACh} channels

Our results indicate that the rapidity of the vagal HR control via the K_{ACh} channels was not affected by background sympathetic tone. In the transfer function, the phase values were significantly more delayed by the K_{ACh} channel blockade in the frequency range from 0.01 to 1 Hz in agreement with our previous study [6]. In contrast, CSS did not affect the phase characteristics, in which no significant interaction was observed at each frequency (Table 2). Moreover, the calculated step response clearly demonstrated that tertiapin significantly prolonged the time constant by >2 s, whereas CSS did not affect it (Fig. 2B and Table 2).

Changes in fitted parameters of the transfer function from vagal stimulation to HR also support our first hypothesis that CSS does not affect the rapidity of the vagal HR control mediated by the K_{ACh} channels. Tertiapin decreased the corner frequency to a similar degree without or with CSS, which did not affect the corner frequency. On the other hand, tertiapin prolonged the lag time, whereas CSS shortened it (Table 3). However, changes in the lag time caused by tertiapin or CSS were less than 0.1 s and might
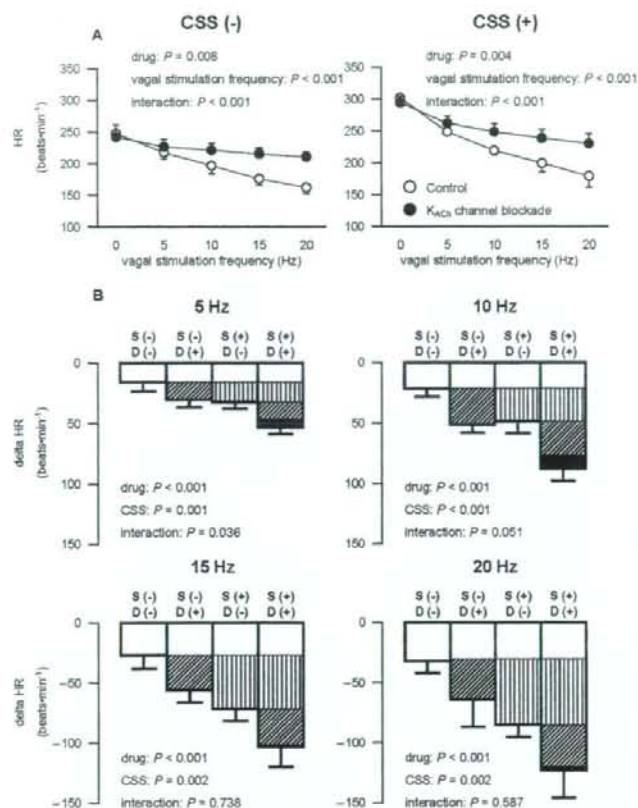
Fig. 3. A: Static HR responses relating stepwise vagal stimulation averaged from all animals (pooled data; $n = 5$) without (left) and with (right) CSS. A K_{ACh} channel blockade decreases the static HR response, and the static reductions in the bradycardic effect were greater at higher stimulation frequencies in both conditions. **B**: Changes in HR responses from baseline to vagal stimulation at 5 Hz (top left), 10 Hz (top right), 15 Hz (bottom left), and 20 Hz (bottom right) averaged from all animals (pooled data; $n = 5$). To aid an intuitive understanding, the tertiapin condition was designated as D(−) in this panel because tertiapin blocked the direct action of ACh. S(+) indicates the presence of CSS. Significant interaction and a tendency towards significant interaction ($P = 0.051$) were obtained at 5 and 10 Hz vagal stimulation, respectively, but not at 15 and 20 Hz vagal stimulation.

be insignificant in terms of physiological HR control.

Effect of CSS on the gain of vagal HR control via K_{ACh} channels

Because the direct action of ACh via K_{ACh} is considered to be independent of sympathetic control [12], an accentuated antagonism is unlikely to occur in the direct action. However, because the interbeat interval is determined by the pacemaker potential of the sinus node cells, which in turn depends on all of the potassium, sodium, and calcium currents, there could be interaction between the K_{ACh} channel pathway and background sympathetic tone when we observe the HR response. Changes in the sodium current and/or calcium current induced by background sympathetic tone would modify the effect of changes in the potassium current through the K_{ACh} channels.

Our results indicate that accentuated antagonism occurred, affecting the direct action of ACh in the range of mild vagal stimulation as follows. In the dynamic protocol that was carried out with a mean vagal stimulation frequency of 5 Hz, significant positive interaction was observed between the tertiapin and CSS effects, affecting the dynamic gain as well as the calculated maximum step

response (Table 2), suggesting that the effect of the K_{ACh} channel pathway was enhanced during CSS. The static protocol also showed significant positive interaction at 5 Hz vagal stimulation (Fig. 3B). The augmentation of the bradycardic response to vagal stimulation gained by the direct action of ACh through the K_{ACh} channels was enhanced under concomitant CSS.

The reason for the absence of a positive interaction between the tertiapin and CSS effects at 15 and 20 Hz vagal stimulation is unclear (Fig. 3B). One possible explanation is the curvilinearity of the HR response to vagal stimulation. In the right panel of Fig. 3A, the tertiapin-free control data (open symbols), which correspond to S(+)D(+) in Fig. 3B, showed the steepest slope at the 0–5 Hz vagal stimulation step. The slope became shallower as the vagal stimulation frequency increased, suggesting a saturation phenomenon of HR reduction in response to vagal stimulation. It is very likely that such curvilinearity masked possible positive interaction between CSS and the direct action of ACh in determining the HR reduction during 15 and 20 Hz vagal stimulation. Accentuated antagonism in the direct action of ACh through K_{ACh} channels might therefore operate under balanced conditions of sympa-

thetic and vagal nerve activities.

The existence of an accentuated antagonism in the direct action of ACh through the K_{ACh} channels could be explained by macromolecular signaling complexes in which G protein-gated inwardly rectifying potassium (GIRK) channels are physically associated with signaling partner regulated by different G protein-coupled receptors (GPCRs) [19, 20]. Cardiac sympathetic stimulation simultaneously activates several different GPCRs: α-adrenergic, β1-adrenergic, and β2-adrenergic receptors. Notably, the β1-adrenergic receptor is coupled to downstream kinase, protein kinase A (PKA). The β-adrenergic signaling via PKA phosphorylation increases the activity of K_{ACh} channels [21, 22]. Taken together, β-adrenergic receptors might augment the activity of K_{ACh} channels via a PKA-dependent mechanism.

Limitations

This study has several limitations. First, the data was obtained from anesthetized animals. Since anesthesia would affect the autonomic tone, the results may not be directly applicable to conscious animals. However, because we cut and stimulated the right cardiac sympathetic and vagal nerves, changes in autonomic outflow associated with anesthesia might not have significantly affected the present results.

Second, we blocked the K_{ACh} channels to examine the effect of background sympathetic tone on the direct effect of ACh through the K_{ACh} channels. On the other hand, if we had blocked the indirect effect of ACh through the cyclic AMP pathway, leaving the direct effect of ACh intact, and then examined the effect of background sympathetic tone on the HR response to vagal stimulation, the results might have been excessively straightforward. However, we could find no blocker for the indirect effect of ACh alone that was suitable for in vivo study at present. Further studies are required to directly examine the effect of background sympathetic tone on the direct effect of ACh through the K_{ACh} channels.

In conclusion, concomitant CSS affected no parameters of rapidity (i.e., the corner frequency in the frequency domain and the time constant in the time domain) of vagal HR control via K_{ACh} channels. Moreover, HR reduction in response to vagal stimulation via K_{ACh} channels was augmented by concomitant sympathetic stimulation at 5 Hz vagal stimulation. These findings suggest that the rapidity of response of the vagal HR control via K_{ACh} channels is invariant with respect to background sympathetic tone, and that the magnitude of vagal HR control via K_{ACh} channels is affected by background sympathetic tone in vivo.

REFERENCES

1. Luetje CW, Tietje KM, Christian JL, Nathanson NM. Differential tissue expression and developmental regulation of guanine nucleotide binding regulatory proteins and their messenger RNAs in rat heart. J Biol Chem. 1988;263:13357-65.
2. Sunahara RK, Dessauer CW, Gilman AG. Complexity and diversity of mammalian adenylyl cyclases. Annu Rev Pharmacol Toxicol. 1996;36:461-80.
3. Huang CL, Slesinger PA, Casey PJ, Jan YN, Jan LY. Evidence that direct binding of G beta gamma to the GIRK1 G protein-gated inwardly rectifying K+ channel is important for channel activation. Neuron. 1995;15:1133-43.
4. Sakmann B, Noma A, Trautwein W. Acetylcholine activation of single muscarinic K+ channels in isolated pacemaker cells of the mammalian heart. Nature. 1983;303:250-3.
5. Yamada M, Inanobe A, Kurachi Y. G protein regulation of potassium ion channels. Pharmacol Rev. 1998;50:723-60.
6. Mizuno M, Kamiya A, Kawada T, Miyamoto T, Shimizu S, Sugimachi M. Muscarinic potassium channels augment dynamic and static heart rate responses to vagal stimulation. Am J Physiol Heart Circ Physiol. 2007;293:H1564-70.
7. Negrão CE, Rondon MU, Tinucci T, Alves MJ, Roveda F, Braga AM, Reis SF, Nastari L, Barretto AC, Krieger EM, Middlekauff HR. Abnormal neurovascular control during exercise is linked to heart failure severity. Am J Physiol Heart Circ Physiol. 2001;280:H1286-92.
8. Mancia G, Grassi G, Giannattasio C, Seravalle G. Sympathetic activation in the pathogenesis of hypertension and progression of organ damage. Hypertension. 1999;34:724-8.
9. Seals DR, Bell C. Chronic sympathetic activation: consequence and cause of age-associated obesity? Diabetes. 2004;53:276-84.
10. Hartzell HC, Méry PF, Fischmeister R, Szabo G. Sympathetic regulation of cardiac calcium current is due exclusively to cAMP-dependent phosphorylation. Nature. 1991;351:573-6.
11. Irisawa H, Brown HF, Giles W. Cardiac pacemaking in the sinoatrial node. Physiol Rev. 1993;73:197-227.
12. Breitwieser GE, Szabo G. Uncoupling of cardiac muscarinic and beta-adrenergic receptors from ion channels by a guanine nucleotide analogue. Nature. 1985;317:538-40.
13. Levy MN. Sympathetic-parasympathetic interactions in the heart. Circ Res. 1971;29:437-45.
14. Kawada T, Ikeda Y, Sugimachi M, Shishido T, Kawaguchi O, Yamazaki T, Alexander J Jr, Sunagawa K. Bidirectional augmentation of heart rate regulation by autonomic nervous system in rabbits. Am J Physiol. 1996;271:H288-95.
15. Kawada T, Uemura K, Kashihara K, Jin Y, Li M, Zheng C, Sugimachi M, Sunagawa K. Uniformity in dynamic baroreflex regulation of left and right cardiac sympathetic nerve activities. Am J Physiol Regul Integr Comp Physiol. 2003;284:R1506-12.
16. Brigham E. FFT transform applications. In: The Fast Fourier Transform and its applications. Englewood Cliffs, NJ: Prentice Hall; 1988. p. 167-203.
17. Bendat J, Piersol A. Single-input/output relationships. In: Random data: analysis and measurement procedures (3rd edition). New York: Wiley; 2000. p. 189-217.
18. Marmarelis P, Marmarelis V. The white noise method in system identification. In: Analysis of physiological systems. New York: Plenum; 1978. p. 131-221.
19. Lavine N, Ethier N, Oak JN, Pei L, Liu F, Trieu P, Rebois RV, Bouvier M, Hebert TE, Van Tol HH. G protein-coupled receptors form stable complexes with inwardly rectifying potassium channels and adenylyl cyclase. J Biol Chem. 2002;277:46010-9.
20. Nikolov EN, Ivanova-Nikolova TT. Coordination of membrane excitability through a GIRK1 signaling complex in the atria. J Biol Chem. 2004;279:23630-6.
21. Kim D. Beta-adrenergic regulation of the muscarinic-gated K+ channel via cyclic AMP-dependent protein kinase in atrial cells. Circ Res. 1990;67:1292-8.
22. Müllner C, Vorobiov D, Bera AK, Uezono Y, Yakubovich D, Frohnwieser-Steinecker B, Dascal N, Schreibmayer W. Heterologous facilitation of G protein-activated K(+) channels by beta-adrenergic stimulation via cAMP-dependent protein kinase. J Gen Physiol. 2000;115:547-58.

Contrasting effects of presynaptic α2-adrenergic autoinhibition and pharmacologic augmentation of presynaptic inhibition on sympathetic heart rate control

Tadayoshi Miyamoto,[1,2] Toru Kawada,[2] Yusuke Yanagiya,[2] Tsuyoshi Akiyama,[3] Atsunori Kamiya,[2] Masaki Mizuno,[2] Hiroshi Takaki,[2] Kenji Sunagawa,[4] and Masaru Sugimachi[2]

[1]*Department of Physical Therapy, Faculty of Health Sciences, Morinomiya University of Medical Sciences; and* [2]*Department of Cardiovascular Dynamics, Advanced Medical Engineering Center, and* [3]*Department of Cardiac Physiology, National Cardiovascular Center Research Institute, Osaka; and* [4]*Department of Cardiovascular Medicine, Graduate School of Medical Sciences, Kyusyu University, Fukuoka, Japan*

Submitted 16 May 2008; accepted in final form 19 August 2008

Miyamoto T, Kawada T, Yanagiya Y, Akiyama T, Kamiya A, Mizuno M, Takaki H, Sunagawa K, Sugimachi M. Contrasting effects of presynaptic α2-adrenergic autoinhibition and pharmacologic augmentation of presynaptic inhibition on sympathetic heart rate control. *Am J Physiol Heart Circ Physiol* 295: H1855–H1866, 2008. First published August 29, 2008; doi:10.1152/ajpheart.522.2008.—Presynaptic α2-adrenergic receptors are known to exert feedback inhibition on norepinephrine release from the sympathetic nerve terminals. To elucidate the dynamic characteristics of the inhibition, we stimulated the right cardiac sympathetic nerve according to a binary white noise signal while measuring heart rate (HR) in anesthetized rabbits ($n = 6$). We estimated the transfer function from cardiac sympathetic nerve stimulation to HR and the corresponding step response of HR, with and without the blockade of presynaptic inhibition by yohimbine (1 mg/kg followed by 0.1 mg·kg^{-1}·h^{-1} iv). We also examined the effect of the α2-adrenergic receptor agonist clonidine (0.3 and 1.5 mg·kg^{-1}·h^{-1} iv) in different rabbits ($n = 5$). Yohimbine increased the maximum step response (from 7.2 ± 0.8 to 12.2 ± 1.7 beats/min, means $\pm$ SE, $P < 0.05$) without significantly affecting the initial slope (0.93 ± 0.23 vs. 0.94 ± 0.22 beats·min^{-1}·s^{-1}). Higher dose but not lower dose clonidine significantly decreased the maximum step response (from 6.3 ± 0.8 to 6.8 ± 1.0 and 2.8 ± 0.5 beats/min, $P < 0.05$) and also reduced the initial slope (from 0.56 ± 0.07 to 0.51 ± 0.04 and 0.22 ± 0.06 beats·min^{-1}·s^{-1}, $P < 0.05$). Our findings indicate that presynaptic α2-adrenergic autoinhibition limits the maximum response without significantly compromising the rapidity of effector response. In contrast, pharmacologic augmentation of the presynaptic inhibition not only attenuates the maximum response but also results in a sluggish effector response.

systems analysis; transfer function; α-adrenergic blockade; rabbits

PRESYNAPTIC α2-ADRENERGIC receptors play an important role in regulating neurotransmitter release in the central and peripheral nervous systems. The concept that neurotransmitter release is modulated by presynaptic autoreceptors was proposed in the 1970s (19, 20, 25, 31–33, 37, 38). Langer (18) first demonstrated that an α-adrenergic antagonist phentolamine, at a concentration below that required to produce its negative chronotropic effect, increases the magnitude of heart rate (HR) response to sympathetic nerve stimulation. Since then, a number of in vivo and in vitro studies have

been conducted to characterize the negative feedback regulation of norepinephrine (NE) release via the presynaptic α2-adrenergic receptors located on the sympathetic nerve terminals (1, 6, 9, 11, 17, 24, 26, 27a, 29, 30, 34, 35). However, the dynamic nature of the presynaptic α2-adrenergic inhibition in sympathetic HR control remains to be quantified. Because we focus on the effector response to sympathetic nerve stimulation, the term "presynaptic" may be interpreted as "prejunctional" throughout this paper to describe more specifically the NE kinetics at the neuroeffector junction.

We first schematize our hypothesis on the possible modes of operations of the presynaptic inhibition. With reference to Fig. 1, the solid and dotted lines indicate the HR responses with and without the presynaptic inhibition, respectively. Figure 1A represents a "limiter-like" operation of the presynaptic inhibition in which the steady-state response is attenuated, while the initial slope of the response is unchanged. Figure 1B represents an "attenuator-like" operation in which the steady-state response is attenuated, while the initial slope of the response is also reduced in proportion to the attenuation of the steady-state response. Since the rapid effector response is one of the important hallmarks of neural regulation compared with humoral regulation, determining which of the two operations likely occurs would contribute to the physiological understanding of the presynaptic inhibition. The words "limiter-like" and "attenuator-like" in this paper are used in the specific senses described above.

To answer which of the two operations likely occurs in the presynaptic inhibition, we examined the HR response to dynamic sympathetic nerve stimulation, with or without blocking the α2-adrenergic receptors in anesthetized rabbits. Because the HR response is mainly mediated by the postsynaptic β1-adrenergic receptors, the administration of an α2-adrenergic receptor antagonist does not eliminate the HR response to sympathetic nerve stimulation. We also examined the effects of pharmacologic augmentation of the α2-adrenergic receptors on the HR response to dynamic sympathetic nerve stimulation. The results of the present study indicated that the presynaptic α2-adrenergic autoinhibition is a limiter-like operation. In contrast, the pharmacologic

---

Address for reprint requests and other correspondence: T. Miyamoto, Dept. of Physical Therapy, Faculty of Health Sciences, Morinomiya Univ. of Medical Sciences, Osaka 559-8611, Japan (e-mail: miyamoto@morinomiya-u.ac.jp).